catalysts

MDPI

Review

Gas-Phase Selective Oxidation of Methane into Methane Oxygenates

Zhen Chao Xu [1] and Eun Duck Park [1,2,*]

[1] Department of Energy Systems Research, Ajou University, Suwon 16499, Korea; zhenchao@ajou.ac.kr
[2] Department of Chemical Engineering, Ajou University, Suwon 16499, Korea
* Correspondence: edpark@ajou.ac.kr

Abstract: Methane is an abundant resource and its direct conversion into value-added chemicals has been an attractive subject for its efficient utilization. This method can be more efficient than the present energy-intensive indirect conversion of methane via syngas, a mixture of CO and H_2. Among the various approaches for direct methane conversion, the selective oxidation of methane into methane oxygenates (e.g., methanol and formaldehyde) is particularly promising because it can proceed at low temperatures. Nevertheless, due to low product yields this method is challenging. Compared with the liquid-phase partial oxidation of methane, which frequently demands for strong oxidizing agents in protic solvents, gas-phase selective methane oxidation has some merits, such as the possibility of using oxygen as an oxidant and the ease of scale-up owing to the use of heterogeneous catalysts. Herein, we summarize recent advances in the gas-phase partial oxidation of methane into methane oxygenates, focusing mainly on its conversion into formaldehyde and methanol.

Keywords: methane; partial oxidation; formaldehyde; methanol; support; promoter

Citation: Xu, Z.C.; Park, E.D. Gas-Phase Selective Oxidation of Methane into Methane Oxygenates. *Catalysts* **2022**, *12*, 314. https://doi.org/10.3390/catal12030314

Academic Editor: Avelina García-García

Received: 17 February 2022
Accepted: 7 March 2022
Published: 9 March 2022

1. Introduction

Petroleum, coal, and natural gas are important fossil fuels and feedstocks for various products, including plastics, clothing, and pharmaceuticals [1]. Coal resources are abundant and broadly distributed worldwide. However, coal mining and utilization have considerable side effects on the ecological environment [2]. The development of the current global economy has been secured by petroleum; nevertheless, its price is unstable and is anticipated to rise steadily owing to its limited reservoir and uneven regional distribution. Therefore, natural gas, a relatively abundant and clean resource among carbon-based resources has attracted growing interest. Its major component is methane, which accounts for approximately 70–90% of its total [3].

In recent decades, substantial methane reserves, including shale gas and gas hydrates, have been discovered. According to the annually published BP Statistical Reviews of World Energy, global natural gas production was 3853.7 billion cubic meters in 2020 [4]. Moreover, methane is the main constituent of biogas, a renewable resource. However, most methane resources are found in sparsely populated areas, such as polar regions and deep sea. Regardless of the mode of transportation, transporting methane to its location of demand is challenging, which inevitably raises its price. Currently, commercial transportation of methane is accomplished through pipelines while liquefied natural gas is shipped. These methods can only be applied to large natural gas reservoirs. Therefore, to utilize a large number of small natural gas wells, the conversion of methane into a more transportable chemical is necessary [5,6].

The present commercial methane conversion technology is based on indirect methane conversion, in which syngas (a mixture of H_2 and CO) is first synthesized via methane steam reforming, methane autothermal reforming, or methane dry reforming reaction, and is subsequently converted into various platform chemicals such as methanol, olefins, aromatics,

and synthetic fuels via well-established C1 chemical processes, including Fisher-Tropsch synthesis [7–9]. Because this process involves an energy-intensive syngas synthesis step, economic benefits are only possible with large-scale processes [10]. Due to its drawbacks, including enormous production costs, massive energy consumption, and high capital costs, the direct conversion of methane into value-added products has attracted much attention as a replacement for the present indirect routes.

Various approaches have been reported for the direct conversion of methane (Figure 1). They can be classified as liquid- and gas-phase reactions. Some routes involve intermediates between methane and its final products. For example, methane halides can first be synthesized from methane and halogen compounds and then further converted into methanol and olefins through hydrolysis and oligomerization, respectively. Under non-oxidative conditions, olefins and aromatic compounds (e.g., benzene, toluene, and xylene (BTX)) can be produced via catalytic or non-catalytic pyrolysis [11]. Even though the operating temperatures are relatively higher because of their thermodynamic limitations, hydrogen can be obtained as a co-product in these processes. Conversely, oxidative coupling of methane is known to directly produce olefins from methane using O_2 [12,13]. We can obtain some value-added methane oxygenates, including methanol and formaldehyde, at moderate temperatures through selective methane oxidation [13–15].

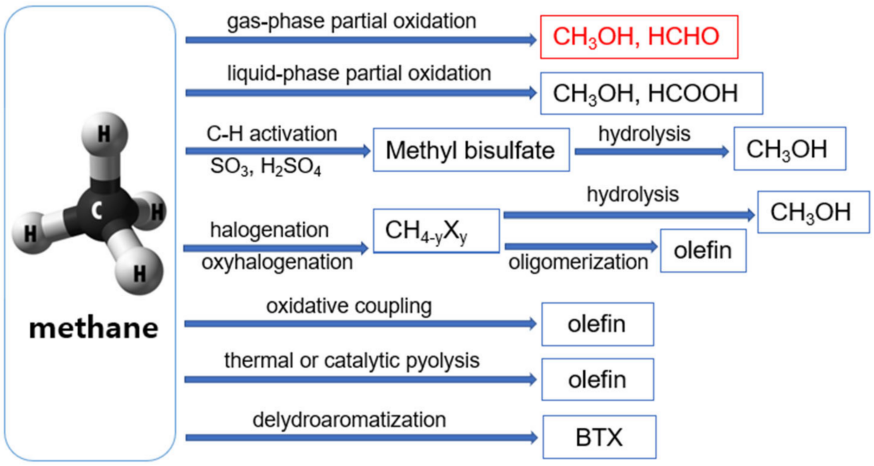

Figure 1. Various routes in the direct conversion of methane technologies.

In the case of partial methane oxidation, there are two problems. First, the C-H bond of methane is so stable that activating it under mild conditions is challenging (Figure 2).

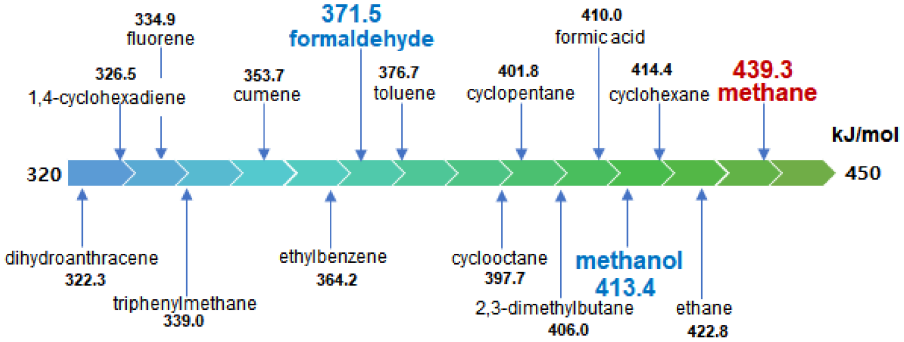

Figure 2. The first dissociation energies for the C-H bond of some hydrocarbons and reaction intermediates during partial oxidation of methane.

Therefore, methane oxidation requires highly reactive reactants or harsh reaction conditions. Second, the C-H bonds of intermediates during methane oxidation are much weaker than those of methane, resulting in low product yields because of over-oxidation of

these intermediates. Generally, the product selectivity decreases with increasing methane conversion for the partial oxidation of methane as well as the oxidative coupling of methane (Figure 3). Therefore, the development of highly active catalysts capable of selectively converting methane into the desired product under mild conditions is necessary for commercializing processes of its direct conversion.

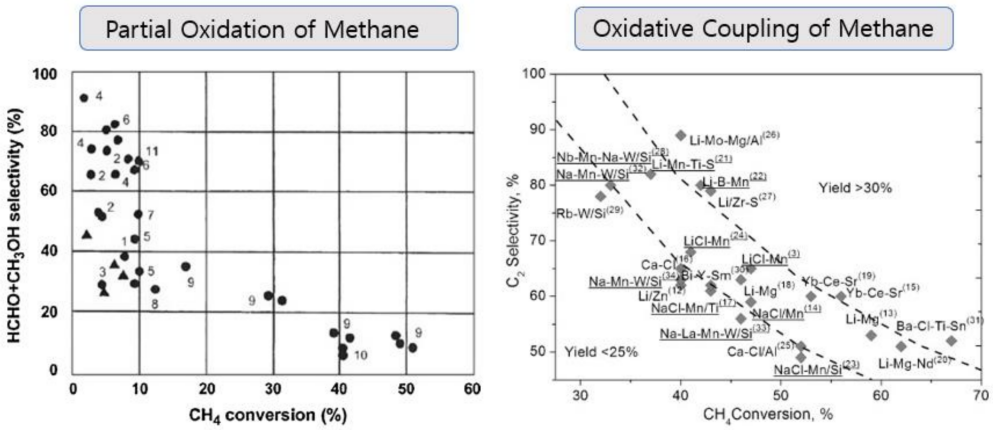

Figure 3. The relationship between product selectivity and methane conversion for partial oxidation of methane [16] and oxidative coupling of methane [17]. Copyright 2011, with permission from Elsevier. Copyright 2011, with permission from Wiley.

Much research has been devoted to the direct partial oxidation of methane, and several available paths are as follows [10].

1. Homogeneous radical gas-phase reaction [18].
2. Liquid-phase selective oxidation reaction [5,19].
3. Heterogeneous gas-phase reaction [20,21].
4. Enzymatic methane oxidation [22].

In the 1970s, Gol'Dshleger et al. [23], first reported the use of homogeneous catalysts for the liquid-phase oxidation of methane into methanol using platinum complexes. Later, sulfuric acid- and trifluoroacetic acid-based systems were developed to achieve a high yield of methanol precursors, such as methyl bisulfate [24] and methyl trifluoroacetate [25], respectively, which needs to be further hydrolyzed into methanol. However, separation of the product is challenging, and the introduction of sulfuric acid and trifluoroacetic acid, which are highly corrosive substances, is not environmentally friendly. To exacerbate to the situation, expensive and highly strong oxidizing agents, such as SO_3 [26,27], $K_2S_2O_8$ [28,29], and H_2O_2 [30] are required to proceed under mild conditions. Compared with liquid-phase methane oxidation, gas-phase reactions over heterogeneous catalysts have the advantages of easy product separation, simple operation, and the potential use of oxygen as an oxidant. Therefore, heterogeneous catalysts have been extensively studied for this purpose. Since methane monooxygenase (MMO) was found to activate methane even under mild natural conditions, the direct activation of methane has been investigated using biomimetic transition metal ions [31], especially iron ions stabilized by zeolite matrices. Although the path for the direct oxidation of methane into methane oxygenates remains meandering, significant progress has been made in the partial oxidation of methane into chemicals, particularly methanol and formaldehyde. Herein, we focus on the recent advances and forthcoming challenges in the gas-phase partial oxidation of methane into methane oxygenates in the past decades. They are classified into two categories based on the product (e.g., formaldehyde and methanol): selective oxidation of methane into formaldehyde and selective oxidation of methane into methanol.

2. Catalytic Gas-Phase Partial Oxidation of Methane into Formaldehyde

Various metal oxides have been reported for the partial oxidation of methane to formaldehyde, which is a thermodynamically favorable exothermic reaction, as shown in Equation (1).

$$CH_4(g) + O_2(g) \rightarrow HCHO(g) + H_2O(g)\ \Delta G^0_{298K} = -281\ \text{kJ/mol},\ \Delta H^0_{298K} = -276\ \text{kJ/mol} \quad (1)$$

Here, we focus on catalysts based on molybdenum, vanadium, iron, and copper oxides. Table 1 summarizes some catalysts used for the gas-phase partial oxidation of methane into formaldehyde in recent decades. Generally, most formaldehyde yields have been reported to be less than 10% and they were obtained with low methane conversions in the temperature range of 450–700 °C. The high formaldehyde yields above 10% were achieved only with relatively high methane conversions over specific V- and Fe-based catalysts.

2.1. Molybdenum-Based Catalyst

2.1.1. Mechanism

MoO_x supported on SiO_2 is one of several most studied catalysts for the partial oxidation of methane to formaldehyde. Since the transition metal Mo can have various oxidation states, it can create a redox cycle between high and low oxidation states. This is required in the Mars-Van Krevelen mechanism, which has been proposed for the selective oxidation of olefins to oxygenates [32–36]. Recent studies have indicated that peroxide species produced by the activation of O_2 on isolated reduced Mo(IV), rather than lattice oxygen are the active species for methane oxidation [37,38]. The kinetics of partial methane oxidation into formaldehyde and structural analysis of the catalyst [37–42] show that multiple molybdenum centers convert methane to formaldehyde. Ohler et al. [43] reported that molybdenum atoms in MoO_x/SiO_2 were isolated pentacoordinate molybdate species containing a single Mo=O bond. One possible mechanism for methane oxidation by isolated MoO_x/SiO_2 is shown in Figure 4. First, the pentacoordinate molybdate species is reduced by H_2, which exists at low concentrations under steady conditions owing to formaldehyde decomposition [44,45], and the oxidation state of molybdenum changes from Mo^{VI} to Mo^{IV}. Furthermore, the reduced molybdenum species were oxidized by oxygen to form oxides. This peroxide then combines with methane to produce HCHO and H_2O, which is a reversible and quasi-equilibrated reaction. Peroxide can also react with H_2 to regenerate primitive molybdenum species. Because the extraction of a proton from the methoxide species formed by CH_4 adsorption is difficult, it is considered to be the rate-determining step for the methane-to-formaldehyde reaction. In contrast, no noticeable change in the Mo K-edge was observed, indicating that the MoO_x species were not reduced by the methane [44]. As H_2O is produced during this catalytic process, it is necessary to discuss the effect of steam on the reaction rate for HCHO synthesis. Outside the dotted line in Figure 4, H_2O exhibited reversible hydrolysis of the Mo-O-Si bond, which may be in quasi-equilibrium under these reaction conditions [46]. Low concentrations of H_2O can positively enhance the rate of formaldehyde generation because of an increase in the concentration of hydroxide groups on the catalyst surface. However, excessive H_2O in the feed hydrolyzes all Mo-O-Si bonds, resulting in the removal of Mo from the silica as volatile $MoO_2(OH)_2$ [46].

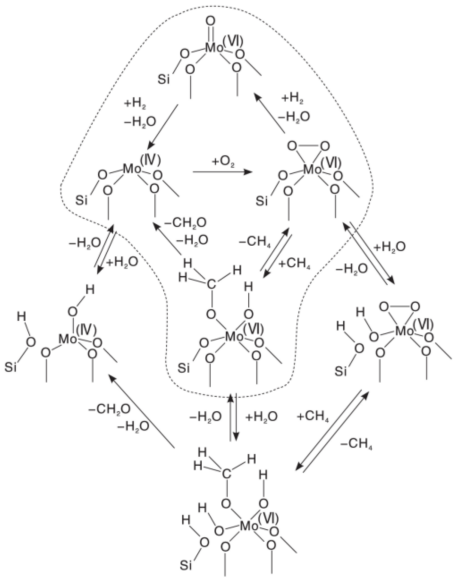

Figure 4. The mechanism of CH_4 oxidation at isolated, SiO_2-supported MoO_x sites, including parallel pathways enabled by the presence of H_2O [43]. Copyright 2006, with permission from American Chemical Society.

Chempath et al. [47] proposed another parallel mechanism through density functional theory (DFT) study, as shown in Figure 5. This mechanism also indicates that the appearance of peroxide species is vital for methane activation, and they considered that the active centers were di-oxo molybdate species (=$Mo(O)_2$). These theoretical results are consistent with the Raman studies of Lee and Wachs [48,49]. Handzlik et al. [50] studied the structure of monomeric molybdenum oxide species in amorphous silica systems using DFT. The results showed that as long as the local structure of silica could be well four-fold bonding to the surface, the monooxo Mo(VI) species would be more stable than the dioxospecies under dehydration conditions, which are rare. Conversely, the majority of positions favor the presence of dioxo Mo(VI) species with two-fold bonding; as such, monooxo Mo(VI) species constitute only a small fraction, which is consistent with other experimental results [48,49,51].

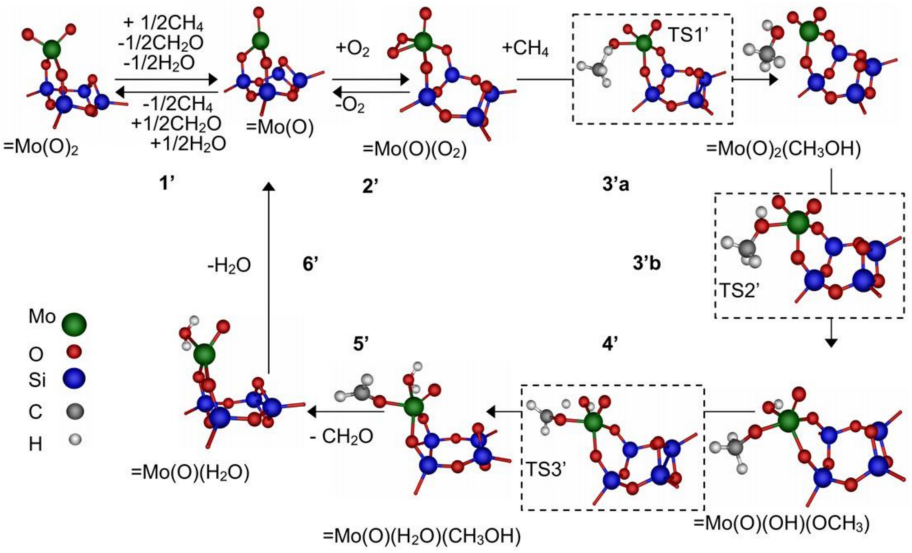

Figure 5. Proposed reaction mechanism based on the assumption of =$Mo(O)_2$ as the active center. Transition state structures are enclosed within dotted lines [47]. Copyright 2007, with permission from Elsevier.

Table 1. Summary of catalysts and their catalytic activity for gas-phase partial oxidation of methane into formaldehyde.

Catalysts	BET Surface (m^2/g)	Active Species Loading (wt%)	T (°C)	CH_4 Conversion (%)	HCHO Selectivity (%)	CO Selectivity (%)	HCHO Yield (%)	GHSV ($mL g_{cat}^{-1} \cdot h^{-1}$)	Ref.
SiO_2	475	/	590	0.10	100	0	0.08	60,000	[52]
WO_3/SiO_2	160	2.0	650	1.2	17	51.3	0.02	5640	[53]
MoO_3	3	/	600	1.0	85	/	0.85	1000–48,000	[54]
MoO_3/SiO_2	/	/	600	8.2	35	17.0	2.9	2800 [b]	[55]
Li-MoO_x/SiO_2	/	1.0	650	4.8	65	0	3.1	5600	[56]
Mo/KIT-6	559	4.6	675	7.3	13	72.9	0.9	36,000	[57]
Mo-KIT-6	569	8.0	675	7.3	29	60.1	2.1	36,000	[57]
eMoO_x/SBA-15	/	20	600	1.9	70	28.0	1.4	33,000	[58]
PMoV-mesoSiO_2	526	3.4	640	5.9	52	/	3.1	36,200	[59]
Mo/ZrO_2	34.3	12	400	8.3	48	17.5	4.0	12,000	[60]
Cu-MoO_x	/	/	700	1.6	62	28.0	1.0	84,000	[61]
Mo-SBA-1	1271	9.9	680	8.2	20	/	/	15,600	[62]
P-MoO_x/SBA-15	382	5.0	675	5.8	90	/	5.2	35,840	[63]
K_2MoO_4/SiO_2	/	2.0	650	1.3	32	21.0	0.42	6000	[64]
V_2O_5/SiO_2	/	/	620	4.8	24	65.0	1.1	3500	[65]
VO_x/MCF-17	750	1.0	600	20	46	24.0	9.2	24,000	[66]
$SiO_2@V_2O_5@Al_2O_3$	14	/	600	22	58	27.0	12.8	24,000	[67]
V/SBA-15	762	1.7	640	4.7	42	/	2.0	480,000	[68]
VO_x/α-Al_2O_3	/	0.4	450	9.0	60	18.0	5.4	10,000	[69]
V/MCM-41	682	2.8	600	4.7	26	/	1.2	180,000	[70]
V/MCM-48	878	2.8	600	4.0	26	/	1.0	180,000	[70]
$FePO_4$	22	/	500	0.51	39	/	0.2	36,000	[71]
$FePO_4$/MCM-41 [a]	310	40	450	3.0	50	/	1.5	7200	[32]
FeO_x/SiO_2	601	0.05	650	5.0	37	39.0	1.9	72,000	[33]
FeO_x/SiO_2	597	/	650	37	33	29.0	12.2	60,000	[34]
CuO_x/SBA-15	617	0.008	625	2.3	58	32.0	1.3	144,000	[35]
B_2O_3/Al_2O_3	/	20	550	6.8	46	50.4	3.1	4650	[36]
SbO_x/SiO_2	237	20	600	1.1	25	52.5	0.28	7840	[72]
Co/SiO_2	333	0.1	500	/	38	/	/	132,000	[73]

[a] The oxidant is N_2O. [b] Space velocity (h^{-1}).

The performance of a supported MoO_x catalyst for the partial oxidation of methane has been reported to be significantly affected by the support, promoter, and preparation method.

2.1.2. Support

Unsupported MoO_3 was first applied to the partial oxidation of methane with little success [74]. Subsequently, due to increasing research on supported catalysts, Mo-based supported catalysts have been studied extensively [53,75–77]. During the 1980s, Liu et al. [78] studied the catalytic performance of MoO_3/SiO_2 for the partial oxidation of methane with N_2O and reported that the selectivity of methane oxygenates was enhanced in the presence of steam because of the formation of $H_4SiMo_{12}O_{40}$, which further limited oxidation of methane oxygenates. Banares et al. [75] reported that the selectivity for formaldehyde varied in a "volcano-type" curve with increasing Mo atom density in MoO_3/SiO_2 catalysts. Molybdenum oxides are not limited to MoO_3; other molybdenum compounds have also been studied. For instance, Erdohelyi et al. [63] investigated the catalytic performance of K_2MoO_4 on different supports. The results showed that the composition of molybdate was closely related to the pH of the slurry containing the support. Low pH values favor $K_2Mo_2O_7$ formation. Moreover, they observed a significant effect of support on the product distribution. Methane conversion was highest when magnesium oxide was used as a support, but no partial oxidation products were observed. In contrast, more formaldehyde was obtained over the catalyst with silica and ZSM-5 as the supports. Therefore, the importance of the support cannot be overlooked because unreasonable selection of a support can contribute to undesired overoxidation of methane. SiO_2 is the best material for formaldehyde formation among SiO_2, Al_2O_3, TiO_2, and various zeolites [48]. Plyuto et al. [79] analyzed the structures of MoO_3/Al_2O_3 and MoO_3/SiO_2 using X-ray photoelectron spectroscopy (XPS) and found that only one type of molybdenum oxide interacted strongly with the alumina surface because a single Mo $3d_{5/2}$-Mo $3d_{3/2}$ doublet shift had higher binding energies than those of bulk MoO_3 in MoO_3/Al_2O_3. In contrast, monomeric or two-dimensional Mo oxides, which are capable of strong electronic interactions with the silica surface, were observed in MoO_3/SiO_2. Thomas et al. [80] indicated that SiO_2 exhibited more pronounced formaldehyde selectivity than Al_2O_3 because of the high rate of successive methane oxidation on alumina. Zhang et al. [59] reported that the methane conversion and selectivity of formaldehyde were related to the density of molybdenum oxide; the higher its density, the higher its catalytic activity for methane conversion. The Mo=O of $Zr(MoO_4)_2$ was reported to be responsible for formaldehyde production, whereas excess lattice oxygen and bulk MoO_3 cause successive oxidation of methane [59].

Since the advent of ordered mesoporous silica, these materials have been used to replace amorphous silica as a support because of their specific properties, including mesoporous structure, large surface area, and high thermal stability [81–83]. Several reports have revealed that MoO_3 and V_2O_5 supported on MCM-41 [69], SBA-1 [61], SBA-15 [84], and KIT-6 [56] have better catalytic activity than MoO_3 and V_2O_5 supported on amorphous silica. The high specific surface area of silica is plausible for the high dispersion of active sites, and its inert surface can facilitate the desorption of the target product, which is essential for avoiding over-oxidation of methane. Pei et al. [58] prepared a mixed-oxide mesoporous silica catalyst (PMoV-mesoSiO_2) using a one-pot method. By controlling the content of the active component and porosity of the mesoporous silica, the highly dispersed catalyst demonstrated adequate selectivity and yield for formaldehyde in the selective methane oxidation reaction. Chen et al. [56] synthesized highly dispersed molybdenum-incorporated (Mo-KIT-6) catalysts through a one-pot hydrothermal synthesis method, which demonstrated very high selectivity for partial oxidation products (nearly 90% total selectivity for CO and formaldehyde), which was explained by molybdenum atoms inserted into the framework of KIT-6 and highly dispersed M=O bonds, leading to high selectivity for formaldehyde. However, for the corresponding supported catalyst (Mo/KIT-6) prepared by the incipient wetness impregnation method, the polymeric MoO_x species and MoO_3 nanoparticles mainly existed on the surface of KIT-6 in the form of Mo-O-Mo bonds,

which could cause the over-oxidation of methane owing to the polymeric MoO_x species, facilitating the decomposition of formaldehyde to generate CO.

2.1.3. Promoter

In addition to the support, the promoter is also an important factor affecting catalytic activity. The promoter can be selected from alkali metals [84–89], phosphorus [62], and transition metals, such as Cu [60], Ti [90], and Ga [51]. The promoter can modify catalyst properties, such as acidity [91], reduction pattern [55], oxygen species [92], and the rate of electron transfer between the adsorbed reactants and catalysts [92]. In most cases, alkali metal promoters poison the catalytic activity owing to geometric blocking of the active center; nevertheless, they can boost the selectivity of methane oxygenates by decreasing the acidity of the support [93]. Moreover, the effect of the promoter may vary depending on its location in the catalyst [92]. Yang et al. [62] used SBA-15 with a larger pore size and higher thermal stability to study the effect of phosphorus as a promoter on the performance of the MoO_x/SBA-15 catalyst and found that phosphorus-modified MoO_x/SBA-15 could increase methane conversion while keeping formaldehyde selectivity unchanged. Liu et al. [94] reported that adding potassium to Mo-KIT-6 catalysts with a low Mo content could improve the catalytic performance for the selective oxidation of propane to acrolein. The addition of potassium to Mo-based catalysts usually alters the structure of the MoO_x active sites [95,96]. When the Mo content is low, increasing the K/Mo ratio contributes to the formation of a distorted Mo-O bond (892 cm^{-1}), implying that K interacts with Mo-KIT-6 to alter its original structure, which promotes selective oxidation.

Inspired by the specific properties of molybdenum oxide, which can be used as a cathode material in lithium-ion battery systems, Kim et al. [55] inserted lithium ions into molybdenum oxide with a silica support to form lithium-molybdenum oxide nanoclusters and redox-driven restructuring of active molybdenum sites to increase the production of formaldehyde significantly. The oxidation state of molybdenum changes owing to the redox migration of Li ions. Under conditions of reduction, lithium ions migrate to molybdenum oxide to produce Li_yMoO_3 nanoclusters. Under oxidation conditions, lithium ions separate from the molybdenum oxide phase to form dispersed MoO_x. The XPS spectra revealed that for the 0.7Li-Mo_x/SiO_2 treated by high-temperature oxidation, the Mo^{5+} component was significantly oxidized to Mo^{6+} compared with the case of MoO_x/SiO_2. For 0.7Li-MoO_x/SiO_2 treated with H_2, the Mo^{5+} component was significantly increased compared to that of MoO_x/SiO_2. Moreover, the Li 1 s XPS spectrum showed that lithium was present in the form of Li_2O after the O_2 treatment. A new binding energy peak appears at 56.2 eV after 0.7Li-Mox/SiO_2 was treated with H_2, indicating that the lithium ions incorporated molybdenum oxide to generate Li_yMoO_3 nanoclusters. Thus, the effective conversion between MoO_x and Li_yMoO_3 led to a significant increase in the formaldehyde yields.

Akiyama et al. [60] prepared the copper-molybdenum complex oxide catalysts (Cu-MoO_x catalysts) for partial oxidation of methane to formaldehyde, which exhibited high selectivity to formaldehyde when water vapor was introduced into the catalytic reaction. In Cu-MoO_x catalysts, the $Cu_3Mo_2O_9$ phase is the active phase for the partial oxidation of methane, which can also restrain the successive oxidation of methane. However, without water vapor, the performance of the Cu-MoO_x catalysts was poor. Developing molybdenum oxide-based catalysts as commercial catalysts remains challenging because of their volatility and the fact that molybdenum oxide transforms into gaseous hydroxide in the presence of water vapor [97].

2.2. Vanadium-Based Catalyst

Vanadium-based catalysts have also been considered promising candidates because they provide relatively higher formaldehyde yields at lower temperatures than molybdenum-based catalysts. Due to the unique catalytic properties of vanadium oxide, vanadium-based catalysts have been comprehensively studied in recent years, with extensive developments

in the fields of oxidative dehydrogenation of short-chain alkanes [98], partial oxidation of methanol [93], and partial oxidation of methane [67].

The difference between the V -and Mo-based catalysts is that methane is directly oxidized to form CO_2 over the Mo-based catalysts [19]. In contrast, methane is first oxidized to formaldehyde, which is then further oxidized to CO_2 over a V-based catalyst under oxidizing conditions [19]. The activity of methane conversion may be strongly related to the isolated dispersed surface metal oxide species, which makes the vanadium oxide species more reactive than molybdenum oxide because of the different nature of the interaction of vanadium oxide with oxygen from that of molybdenum oxide [99]. Moreover, V_2O_5 was more stable than MoO_3. Therefore, V-based catalysts are expected to replace Mo-based catalysts for the selective oxidation of methane to formaldehyde.

2.2.1. Mechanism

Many studies on the different oxidation reactions over V-based catalysts have shown that monomeric and polymeric surface VO_4 species in supported vanadium catalysts are usually active sites because there are a few exposed active surface sites in the crystalline phases [100–102]. Raman spectroscopy and in situ infrared (IR) analysis revealed that only one terminal V=O bond existed in the dehydrated surface VO_4 species [48].

In the isolated VO_x tetrahedron, the V=O bond is considered to be the active site, while the surface VO_x species without the V=O bond would cause the formation of successive oxidation products; however, it has also been suggested that the bridging V-O-Si bonds may also be involved in the catalytic reaction, and that a large number of Si-OH groups on the surface of the catalyst also participated in the redox process of the active site, extracting the H atoms from the CH_4 molecule to stabilize the V^{4+}=O center [103]. Ding et al. [104] investigated the gas-phase reaction of methane with V-Si heteronuclear oxide clusters using DFT calculations and mass spectrometry experiments. They pointed out that there is a terminal oxygen-centered radical O_t· in the stoichiometric clusters $[(V_2O_5)_n(SiO_2)_m]^+$, which can extract an H atom from methane to form a methyl radical, as shown in Equation (2). Hydrogen capture is thermodynamically and kinetically favorable. Therefore, the O_t· radical was deemed to activate methane in the stoichiometric cluster. Interestingly, the authors noted that the O_t· radical in the stoichiometric cluster was connected to the Si atoms instead of the V atoms [103].

$$[(V_2O_5)_n(SiO_2)_m]^+ + CH_4 \rightarrow [(V_2O_5)_n(SiO_2)_mH]^+ + \cdot CH_3 \quad (2)$$

The acidity of the surface vanadia species is also important for catalytic performance. Typically, oxide supports have only surface Lewis acid sites, and the relative intensity of the acid sites is $Al_2O_3 > TiO_2 > ZrO_2$. However, for SiO_2, no surface Lewis acid sites were detected [105]. IR investigation indicated that methane can be adsorbed onto SiO_2 via hydroxyl groups or coordinatively unsaturated lattice oxygen, and the T_d symmetry of methane is distributed during adsorption, similar to that of basic oxides [5]. In contrast, there are both surface Lewis and Brønsted acid sites in the crystalline powders of V_2O_5, and the ratio of Brønsted and Lewis acid sites increases with the loading of vanadia [106]. Hu et al. [107] determined the acidity of V-SiO_2 catalysts by NH_3-TPD measurements and showed that all V-SiO_2 catalysts contained weak acid sites corresponding to monomeric or low-polymerized VO_x species [108].

Decreasing the reaction temperature while maintaining the methane conversion to increase the yield of methane oxygenates is more effective because nonselective oxidation can be dominant at high temperatures. Ghampson et al. [109] achieved selective oxidation of methane at low temperatures (300–400 °C) with O_2 using a NO/NO_2 oxygen atom shuttle over vanadium oxide catalysts and suggested possible reaction pathways, as shown in Figure 6. Isolated vanadium species with three bridging siloxy bonds interact with NO_2 to generate a monodentate nitrate species, which can be rearranged to a reactive bidentate nitrate; moreover, when the bidentate nitrate combines with methane, NO and methoxy species are released, which can hydrogenate with vanadium to form formaldehyde through

electron rearrangement [109]. Some studies have suggested that NO may act as a free radical initiator to facilitate the gas-phase reaction, and the conversion between NO and NO_2 drives the transfer of oxygen atoms for the partial oxidation of methane [110,111].

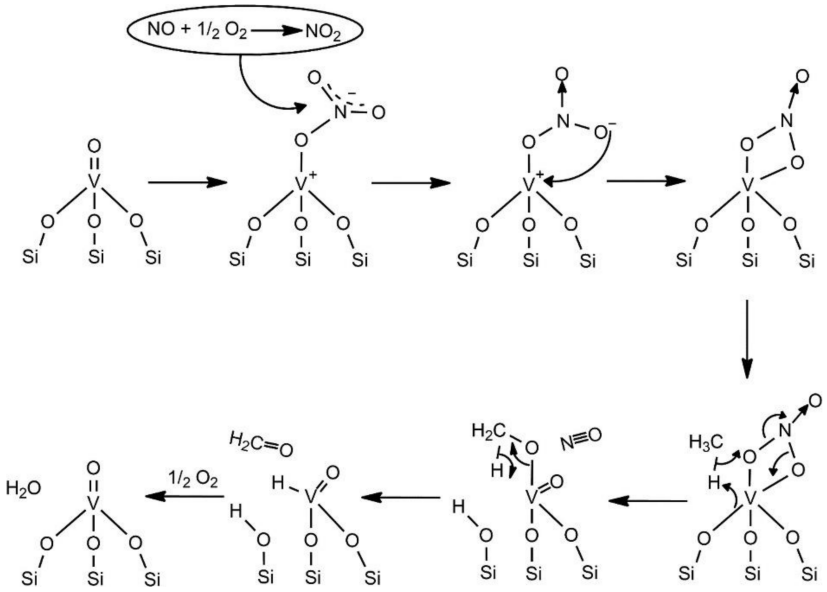

Figure 6. Possible scheme for the formation of HCHO during the CH_4 partial oxidation by NO + O_2 involving the terminal V=O bond and the Si-O-V bond [109]. Copyright 2021, with permission from Elsevier.

2.2.2. Support

In the previous section, we mentioned that the highly dispersed VO_x species are active for the partial oxidation of methane. Although TiO_2, ZrO_2, and Al_2O_3 are common supports for supported catalysts, with increasing VO_x loading or after high-temperature calcination, vanadia is mainly present as polyvanadate species. It was demonstrated that bulk vanadia would be present in VO_x/α-Al_2O_3, decreasing both the activity and selectivity during the partial oxidation of methane [68], but not when SiO_2 is used as a support. Arena et al. [112] reported that when TiO_2 was used as a support, the main product was CO, and its ability to activate methane was lower than that of SiO_2. Therefore, many studies have been devoted to studying vanadium catalysts with ordered mesoporous silica supports, such as MCM-41 [69], MCM-48 [69], SBA-15 [67,113], and MCF-17 [65].

A possible pathway for the formation of the active site and its interaction with methane and oxygen is proposed (Figure 7). To optimize the partial oxidation of methane to formaldehyde over the V-MCM-41 catalysts, Du et al. [114] developed a statistical model using an appropriate experimental design. This statistical model provided a reasonable prediction of methane conversion, formaldehyde selectivity, and space-time yield, and showed that temperature, the feed ratio of methane to oxygen, and pressure were the most critical factors affecting formaldehyde selectivity. Therefore, Dang et al. [115] explored the influence of V sources on the catalytic performance of VMCM-41. They found that when $VO(acac)_2$ was used as VMCM-41 precursor, mainly VO_x monomers were generated, while $VOSO_4$ as VMCM-41 precursor, oligomeric VO_x species were formed. The highly dispersed VO_x monomer enhanced formaldehyde selectivity. The space-time yield of formaldehyde reached 5.3 $kg_{CH2O} \cdot kg_{cat}{}^{-1} \cdot h^{-1}$ at 873 K, which was significantly better than that of the VMCM-41 catalyst prepared with $VOSO_4$ as the vanadium source [115].

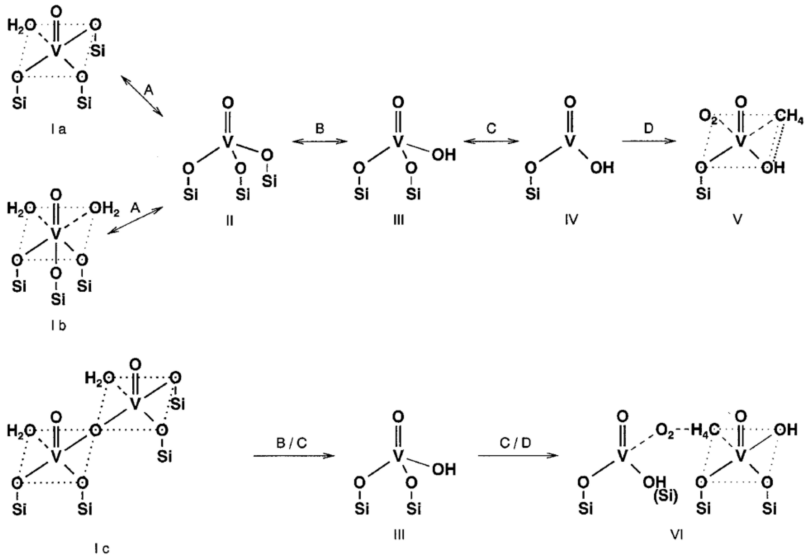

Figure 7. Scheme of the formation of the active sites and their interaction with O_2 and CH_4: (Ia,b) coordinatively saturated V^vO_x species in the stored catalyst, (Ic) bridged V^vO_x species in the catalyst, (II) isolated V^vO_x species, (III) acidic V^vO_x species, (IV) acidic $V^{IV}O_x$ species, (V) adsorption complex of O_2 and CH_4 on one active species, (VI) adsorption complex on neighboring "reduced site" and acid site, (A) reversible dehydration, (B) partial hydrolysis by water formed, (C) reduction to $V^{IV}O_x$ species under catalytic condition, (D) coordination and activation of O_2 on a V^{IV} site and of CH_4 on an acidic V^{IV} or V^V site [69]. Copyright 2000, with permission from Elsevier.

Most preparation methods described in the literature involve the wet impregnation of SiO_2. However, because the aqueous solution of silica is acidic, this causes the vanadium species to exist in a multi-nuclear form, which is not beneficial for forming dispersed vanadium species. To form highly active and selective isolated species of V, Nguyen et al. [103] used mononuclear precursors to prepare a series of V-based catalysts. The results showed that in the more active catalysts, there are more silanol groups that may participate in the redox process of the active site, making it possible for the vanadium oxide center (V^{4+}-O^-) to extract H atoms from methane. In the reaction process of traditional supported V-based catalysts, the dispersed VO_x species may be gradually polymerized, resulting in a decrease in the performance of the catalyst. Yang et al. [66] prepared novel SiO_2@V_2O_5@Al_2O_3 core-shell catalysts via hydrothermal synthesis followed by atomic layer deposition (ALD). After 50 ALD cycles, the core-shell catalyst exhibited the best catalytic activity. Methane conversion and formaldehyde selectivity were as high as 22.2% and 57.8%, respectively. The catalyst remained active for 35 h reaction, which is attributed to the formation of new tetrahedral monomeric vanadium species and V-O-Al bonds during the ALD process.

Ordered hexagonal mesoporous pure silica SBA-15 has been regarded as a promising support for supported catalysts. Fornés et al. [84] synthesized the first VO_x/SBA-15 catalyst for partial oxidation of methane. They indicated that due to the high specific surface area of the SBA-15 material, the monolayer capacity would reach a higher V loading than that in amorphous silica. Wallis et al. [113] explored the effects of morphology and pore structure on the performance of VO_x/SBA-15 by varying the aging temperature. It was observed that an optimum aging temperature (e.g., 70 °C) contributed to the formation of more monomers and lower oligomeric VO_x species on SBA-15, thus outperforming the catalytic performance of the other two samples.

Kunkel et al. [116] used an artificial neural network modeling to enhance the catalytic performance of V-SBA-15. The results showed that the pH significantly affected the catalyst activity during catalyst preparation. Methane conversion and formaldehyde selectivity were highest at pH 2.5. After analyzing over 200 samples, the artificial neural network

modeling was used to obtain the optimal response parameters and ultimately an excellent space-time yield of 13.6 $kg_{CH2O} \cdot kg_{cat} \cdot h^{-1}$ [116]. The higher the temperature and partial pressure of water in a given temperature range, the greater the conversion of methane. However, lower partial pressures of water would more significantly inhibit formaldehyde oxidation. Therefore, the active sites leading to methane activation and formaldehyde oxidation are different [67]. Yang et al. [65] compared the effect of supports (SBA-15 and MCF-17) on the catalytic oxidation of methane to formaldehyde. Compared with SBA-15, MCF-17 has a larger specific surface area and a more pronounced mesoporous structure, resulting in higher methane conversion over VO_x/MCF-17.

2.2.3. Promoter

Few reports on the effect of the promoter in V-based catalysts on the partial oxidation of methane exist. The Sb-V-O/SiO_2 catalyst was reported to be better than single metal oxide catalysts, such as VO_x/SiO_2 and SbO_x/SiO_2, in terms of formaldehyde yield [117]. Formaldehyde yields of up to 3% were achieved at 650 °C with the Sb-V-O/SiO_2 catalyst; moreover, the Sb/V ratio also influences the catalyst performance owing to the phase transformation of the Sb-V mixed oxide [117]. Wallis et al. [90] prepared V/Ti-SBA-15 catalysts and found that the Ti promoter contributed to the dispersion and reduction of the VO_x species, thereby increasing the activity of the catalyst. Shimura et al. [51] comparatively investigated the effect of promoter (Ga) incorporation on catalytic performance. They showed that V(2–3 wt%)/Ga(0.1–0.5 wt%)/SiO_2, prepared by sequential impregnation, had the highest formaldehyde yield at 863 K.

2.3. Iron-Based Catalyst

Iron has been extensively studied because of its excellent catalytic properties and price advantages, especially since it was revealed that zeolites, such as mordenite and ZSM-5, are capable of stabilizing dinuclear iron centers in a form similar to that found in MMO [118,119]. On the surface of transition metal oxides, isolated active lattice oxygen atoms are favorable for suppressing the over-oxidation of intermediates during methane oxidation [40]. Therefore, the design and preparation of catalysts with isolated active sites can efficiently improve formaldehyde yield. However, the structure and nature of the active sites are strongly influenced by active metal loading, preparation method, support, and promoter.

Kobayashi et al. [120] found that highly dispersed tetrahedrally coordinated Fe^{3+} species on SiO_2 could significantly boost formaldehyde yields. A study on the effects of direct hydrothermal synthesis (DHT) and template-ion exchange (TIE) methods on the catalytic performance of Fe-MCM-41 catalysts revealed that the DHT method resulted in isolated tetrahedrally coordinated Fe-O species within the support skeleton, whereas the catalysts prepared by the TIE method provided predominantly polymeric, octahedrally coordinated iron oxide clusters. Therefore, Fe-MCM-41 prepared by the DHT method exhibited higher catalytic performance [121]. These studies further indicate that for obtaining high formaldehyde selectivity, highly dispersed Fe sites are vital. However, there is no consensus regarding the structure of the active Fe species. Therefore, it is of great significance to further modify FeO_x-SiO_2 to boost its catalytic performance and investigate the relationship between its structure and catalytic performance.

The sol-gel method can be used to prepare supported catalysts with evenly distributed active phases [122]. Therefore, He et al. [123] prepared the FeO_x-SiO_2 by the sol-gel method and found it to be more active than the catalysts prepared by the impregnation method. Moreover, they noted that the strong interaction between iron and phosphorus in the P-FeO_x-SiO_2 catalysts resulted in the formation of $FePO_4$ nanoparticles. The peculiar structure of iron, tetrahedral Fe^{3+} isolated by phosphate groups, in the $FePO_4$ nanoclusters contributes to enhancing the selectivity of formaldehyde, and the one-pass yield of formaldehyde over the P-FeO_x-SiO_2(P/Fe = 0.5) catalyst up to 2.4% at 898 K, which is consistent with studies showing that the support of $FePO_4$ onto SiO_2 boosted the conver-

sion of methane [124,125]. Further research has shown that in the process of preparing FeO_x-SiO_2 by the sol-gel method, the pH affects the dispersion of the active species on the silica, and a low pH value leads to an increased product yield [126]. Moreover, metal phosphates have unique acid-base properties allowing them to be used not only for the oxidative coupling of methane but also for efficient acetalization reactions; therefore, the surface acid-base properties of $FePO_4$ are also critical for determining the selectivity for methane oxidation [127,128]. Thus, Matsuda et al. [70] proposed a possible mechanism for methane oxidation by investigating the effect of redox and acid-base properties on the surface of various types of crystalline Fe-based phosphates as well as oxide catalysts, as shown in Figure 8. The use of methane as a reducing agent and oxygen as an oxidizing agent allows the catalyst to convert between two forms, $FePO_4$ and $FePO_{4-\delta}$, creating a catalytic cycle that produces a continuous stream of formaldehyde. The Lewis acid and weakly basic sites of $FePO_4$ are responsible for the activation of C-H, which directly contributes to the formation of formaldehyde. Further studies have shown that in the steady state, this kind of cycle is not involved in the catalytic process and that methane is oxidized on the surface of $FePO_4$, maintaining the morphological structure of $FePO_4$. A possible mechanism for the direct oxidation of methane by Fe_2O_3 to produce CO_2 is shown in Figure 8, which is similar to that described above. However, this explanation is the exact opposite of the conclusions of Krisnandi et al. [129]. They concluded that the Fe_2O_3/NaY catalyst could oxidize methane to formaldehyde, even when the selectivity of formaldehyde exceeded 80%. Therefore, the mechanism and active sites of Fe-based catalysts for the selective oxidation of methane to formaldehyde remain controversial, and further research is needed.

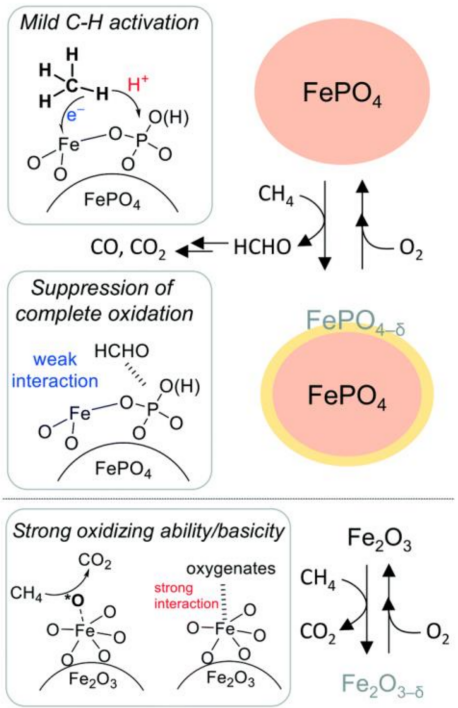

Figure 8. Proposed reaction mechanism for the oxidation of CH_4 over $FePO_4$ into HCHO with O_2 using $FePO_4$-MA and complete oxidation of CH_4 over Fe_2O_3 into CO_2 with O_2 using Fe_2O_3 [70]. Copyright 2021, with permission from Royal Society of Chemistry.

Due to the confined effect of the ordered mesoporous channels, the growth of highly dispersed Fe species and FeO_x nanoclusters toward Fe_2O_3 particles is limited [33]. Thus, SBA-15 is a promising support for preparing more efficient Fe-based catalysts. Zhang et al. [33] investigated the catalytic behavior and kinetic features of FeO_x/SBA-15. These results suggest that the selectivity of formaldehyde decreases with increasing Fe content.

Structure–performance correlation and pulse reaction studies clarified that crystalline Fe_2O_3 accounted for the complete oxidation of methane. The lattice oxygen is not relevant to the formation of formaldehyde, as the products are only CO and CO_2, similar to the Mo-based catalyst. Furthermore, metal phosphates have received considerable attention [128,130–133], and optimized catalyst design and process modifications may enable these metal salts to becoming promising alternatives to metal oxide catalysts.

2.4. Copper-Based Catalyst

Copper has been intensively studied as the active center of particulate methane monooxygenase in methanogenic bacteria, and has received extensive attention concerning the catalytic partial oxidation of methane with O_2 [134–138]. Li et al. [35] studied the catalytic behavior and mechanism of CuO_x/SBA-15 for the selective oxidation of methane by oxygen, as shown in Figure 9. The Cu loading had a considerable effect on the performance of the catalyst. CuO_x/SBA-15 with a copper content of 0.008 wt% exhibited the best specific site rate for formaldehyde formation, 5.6 mol (mol Cu)$^{-1}$s^{-1}). The lattice oxygen linked to Cu interacts with methane to directly produce CO and CO_2. Simultaneously, Cu^{II} is reduced to Cu^{I}, which acts as the active center for the activation of O_2, forming active oxygen (O*) and accounting for the selective conversion of methane to formaldehyde. Thus, the lattice oxygen is not the active oxygen species for producing formaldehyde, but is essential for the system because a certain amount of methane typically has to be foregone to reduce Cu^{II}. In other words, in this system, formaldehyde production is accompanied by CO_x generation at all times. Therefore, we can achieve a significant increase in formaldehyde selectivity by optimizing the catalyst preparation process and eliminating the effects of lattice oxygen.

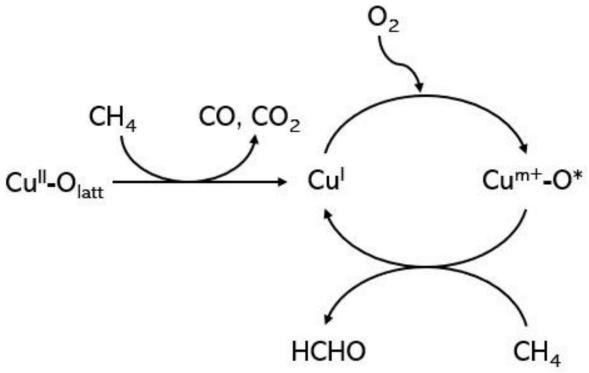

Figure 9. Reaction mechanism for selective oxidation of CH_4 to HCHO over the CuO_x/SBA-15 catalyst [35]. Copyright 2008, with permission from American Chemical Society.

An et al. [139] studied CuO_x/SBA-15 and determined that the activity of CuO_x/SBA-15 prepared using the grafting approach was significantly higher than that of CuO_x/SBA-15 prepared using the impregnation method, which seems to be closely related to the proportion of Cu^{II} in each catalyst at low Cu loadings.

2.5. Other Catalysts

In addition to the aforementioned types of catalysts, other transition metal and nonmetal catalysts have also attracted attention. Chemical similarities between WO_3 and MoO_3 overlayers in silica-supported catalysts have been reported [140,141]. In addition, De Lucas et al. [52,142] investigated the catalytic properties of W/SiO_2 for partial oxidation of methane to formaldehyde. The terminal W=O sites would lead to formaldehyde formation, and the W-O-W bridging functionalities cause complete oxidation of CH_4 and CO. Moreover, the introduction of potassium resulted in higher C2 hydrocarbon yields [52]. Cobalt-containing zeolites have broad application prospects, and the form of Co determines the selectivity and activity of Co-ZSM-5 [143]. The enhanced selectivity of formaldehyde

after acid treatment of ZSM-5 by Beznis et al. [144] was attributed to the increased amount of Co^{2+} in the ZSM-5 channel, which was responsible for the generation of formaldehyde. Recent studies have shown that non-metallic boron-based catalysts exhibit outstanding catalytic performance in dehydrogenation [145,146]. Based on this finding, Tian et al. [36] reported that B_2O_3 catalysts were highly stable and selective for the partial oxidation of methane to HCHO and CO. The mechanism of methane activation on a B_2O_3 surface adequately explains the generation process of HCHO and CO, as shown in Figure 10, which reveals that molecular O_2 is bound to the electron-deficient B centers on the B_2O_3 surfaces which are moderate oxidants accounting for methane activation and suppress the formation of CO_2.

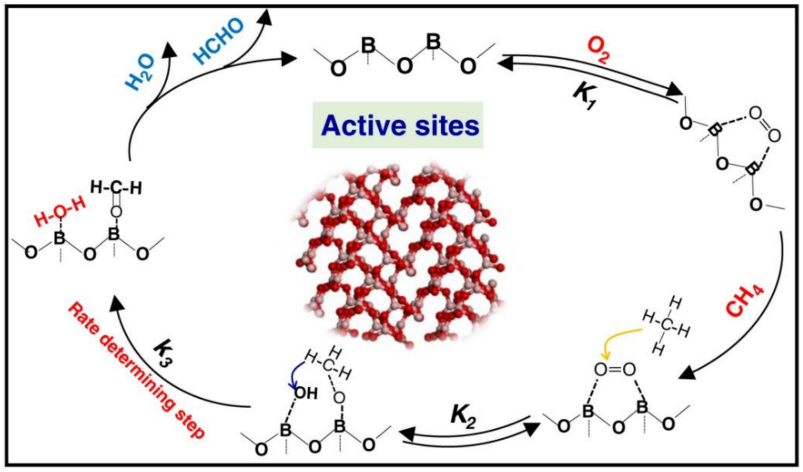

Figure 10. Schematic diagram of the plausible pathway of partial oxidation of methane to formaldehyde on B_2O_3 catalysts [36]. Copyright 2020, with permission from Nature.

3. Catalytic Gas-Phase Partial Oxidation of Methane into Methanol

From a thermodynamic viewpoint, the selective oxidation of methane into methanol can proceed spontaneously even at room temperature (Equation (3)). However, methanol is more reactive than methane and susceptible to over-oxidation leading to CO and CO_2. Therefore, the design of catalysts with high activity and selectivity and the adoption of specific methanol protection methods are critical measures for improving methanol yield. Herein, we discuss heterogeneous catalysts based on molybdenum, vanadium, iron, and copper. Some of the catalytic activity data for the partial oxidation of methane to methanol are presented in Table 2.

$$CH_4(g) + 1/2O_2(g) \rightarrow CH_3OH(g)\ \Delta G^{o}_{298K} = -111\ \text{kJ/mol},\ \Delta H^{0}_{298K} = -126\ \text{kJ/mol} \quad (3)$$

3.1. Molybdenum-Based Catalyst

Atroshchenko et al. [147] discovered that MoO_3 can catalyze the partial oxidation of methane into methanol at high temperatures and pressures. Dowden et al. [148] reported that loading MoO_3 onto a support could improve the catalytic performance of this reaction. The most active catalyst (Fe_2O_3 (MoO_3)) permitted methanol productivity of up to 869 $g{\cdot}kg^{-1}{\cdot}h^{-1}$ methanol at 5 MPa and temperatures of 703–773 K [148]. Zhang et al. [149] comparatively studied the effects of ZrO_2 and La-Co-O as supports on the selective oxidation of methane to methanol over a MoO_3 catalyst. MoO_3/ZrO_2 only catalyzed methane to produce traces of methanol, the main product being formaldehyde, while 7 wt% MoO_3/La-Co-O enabled the conversion of methane up to 11.2% and methanol selectivity up to 60%. The characterization results showed that molybdenum oxide in the amorphous state was well dispersed on the catalyst surface, and there was no crystal phase or molybdate. More importantly, the authors indicated that proper reducibility and O^-/O^{2-} ratios favored methanol production, which is consistent with Liu et al. [78]. The presence of steam in the

reaction atmosphere affects the performance of the catalyst. Sugino et al. [150] reported that molybdate ($H_4SiMo_{12}O_{40}$) was formed on the SiO_2 surface as the amount of steam increased, which inhibited the deep oxidation of products such as CH_3OH, indicating that the catalytic performance of MoO_3 prepared by the sol-gel method was superior to that of the impregnation method. At 873 K, methane conversion and methanol selectivity were 8.2% and 11%, respectively [150].

Table 2. Summary of catalysts and their catalytic activity for continuous gas-phase partial oxidation of methane into methanol.

Catalysts	T (°C)	Oxidant	CH_3OH Productivity ($mmol/mol_{metal}/h$)	CH_3OH Selectivity (%)	Ref.
Mo/SiO_2	600	$N_2O + H_2O$	0.36 [a]	60	[151]
MoO_x/La-Co-O	420	O_2	/	60	[149]
V_2O_5/SiO_2	460	O_2	0.55 [a]	34	[152]
Cu/CHA	300	$H_2O + O_2$	542	91	[153]
Cu/CHA	270	$H_2O + O_2$	26	53	[154]
Cu-H-MOR	400	$H_2O + O_2$	143	99	[155]
Cu-H-MOR	350	H_2O	29	100	[155]
Cu-Fe/Al_2O_3	450	$H_2O + O_2$	1.3 [a]	/	[156]
Fe-Cu-BEA	270	$N_2O + H_2O$	0.26 [a]	72	[157]
Rh-dB-ZSM-5	150	$O_2 + H_2O + CO$	0.80 [a]	44	[158]
NiFeO/CZ	250	H_2O	3.2×10^{-3} [a]	1.24	[159]
Cu-SSZ-39	325	$N_2O + H_2O$	1044	34	[160]
Cu-MOR	350	H_2O	332	/	[161]
ZnO/Cu_2O/Cu	177	$H_2O + O_2$	7.02×10^{17} [b]	87.5	[162]
Cu-CHA	300	$H_2O + O_2$	0.68 [a]	45	[163]

[a] CH_3OH yield ($mmol_{CH3OH}/g_{cat}/h$). [b] CH_3OH yield (molecules cm^{-2} s^{-1}).

3.2. Vanadium-Based Catalyst

In Section 2, we stated that promoters, supports, preparation methods, and loading are crucial parameters affecting the performance of V-based catalysts for the partial oxidation of methane and directly determine the structure and properties of the active vanadium species [152]. The methanol selectivity of the 8 wt% vanadium catalyst was only 6.8%, whereas that of the 2 wt% vanadium catalyst reached 57% [152]. It has been reported that radical production may be one of the factors controlling methane conversion [164]. Barbero et al. [110] added NO to the feedstock, which changed the CH_3-CH_3O_2 radical ratio and thus promoted methane activation because the introduction of NO may trigger the chain propagation of the radical reaction. The yields of CH_3OH and HCHO reached 16% in the presence of 1% NO in the feed solution [110]. The selectivity for methanol decreased with increasing vanadium loading, owing to the influence of the vanadium oxide size [152].

3.3. Iron-Based Catalyst

In recent years, the focus of research has shifted from vanadium- and molybdenum-based catalysts to iron- and copper-containing zeolites [165–168]. To achieve efficient conversion of methane at low temperatures, researchers expect to prepare metal molecular sieve catalysts by mimicking MMO to form active binuclear Fe or Cu centers [169–174]. In general, Fe-zeolite catalysts require N_2O to effectively activate methane [167,175]. The surface oxygen generated by N_2O played a key role in both CO and CH_4 oxidation. Further studies elaborated on the reaction process, as shown in the following equations, and suggested that this surface oxygen species, α-O, leads to methoxy and hydroxy groups bound to α-sites [176].

$$N_2O + (Fe^{II})\alpha \rightarrow (Fe^{III} - O^-)\alpha + N_2 \quad (4)$$

$$CH_4 + (Fe^{III} - O^-)\alpha \rightarrow (Fe^{II} - CH_3OH)\alpha \quad (5)$$

$$(Fe^{II} - CH_3OH)\alpha \rightarrow (Fe^{II})\alpha + CH_3OH_{ads} \quad (6)$$

Eugeny et al. [177] confirmed by IR spectroscopy that the surface reaction of CH_4 and α-O proceeds through a hydrogen extraction mechanism. Magnetic circular dichroism suggests that α-Fe(II) is a mononuclear, high-spin, square-planar Fe(II) site [178]. The reaction of this species with the oxygen atom in N_2O forms a mononuclear, high-spin Fe(IV)=O species, whose exceptional reactivity is derived from a constrained coordination geometry effect on the zeolite lattice [178]. Bols et al. [179] increased the percentage of α-Fe (II) in the total Fe species to 72%, which was attributed to the one-pot synthesis strategy that enabled the well-dispersed mononuclear iron cations into the zeolites. Characterized by variable-temperature Mössbauer, diffuse reflectance UV-vis-NIR, and Fourier transform IR spectroscopy, weak Fe-N_2O interaction facilitates isomerization to the O-bound form at higher temperatures, resulting in O-atom transfer. However, at lower temperatures, N_2O enables numerous backbonds by binding terminal nitrogen atoms to Fe(II) centers [180]. Very recently, Snyder et al. [181] studied the cage effects on methane hydroxylation in zeolites in detail, and indicated that the local pore environment of heterogeneous active sites was a critical factor in selecting the reaction pathway with a low activation barrier, which was verified by comparing the local environments of α-Fe(IV)=O sites in BEA and CHA, in which the constricted pore apertures of CHA promoted selective hydroxylation and precluded deactivating side reactions.

Comparing the performance of the three catalysts, Fe-ZSM-5, Fe-Beta, and Fe-FER, Fe-FER is the most active catalyst for methane conversion because numerous framework Al atoms in H-FER are essential for the generation of active extra-framework Fe species [182]. Fe-ZSM-5 is significantly deactivated owing to coke formation, which is believed that the low Lewis acidity and small pore size would accelerate the methanol to olefin reaction to form coke [182]. Parfenov et al. [183] reported that the addition of steam to feedstock significantly inhibited coke formation and boosted methanol selectivity. More importantly, they indicated that methanol generated by α-O oxidation then migrated from the α-sites, initiating new reaction cycles, which was the first to find the cut-off point between the quasicatalytic and catalytic modes in the same system. Electron paramagnetic resonance (EPR) spectra and UV-vis spectra results demonstrate that by increasing the content of extra-framework Al, the proportion of iron in tetrahedral or octahedral coordination increases, while the clustered Fe species decreases, which is responsible for the increase in methane conversion and methanol yield [184]. Moreover, Zhao et al. [185] reported that modification of the CH_4/N_2O ratio could balance coke formation and deep oxidation to optimize the generation of the desired products.

By mimicking the structure of enzymes catalyzing selective oxidation at low temperatures, Simons et al. [186] studied the conversion of methane to methanol with N_2O catalyzed by Fe(II) sites within Fe_3-μ_3-oxo nodes in the metal-organic frameworks (MOFs). The selectivity of methanol was improved by adding protonic zeolite in the MOF because methanol generated on Fe(II) sites could be protected from over-oxidation in the presence of zeolitic Brønsted acid groups.

3.4. Copper-Based Catalyst

Although the attribution of the active species in Cu zeolite catalysts remains controversial, unlike Fe zeolite catalysts, Cu zeolite catalysts can directly oxidize methane to methanol with O_2 [27,166,187,188]. Figure 11A demonstrates the proposed various copper active species formed inside the zeolite pores, such as monovalent copper oxygen species attached to one zeolite framework Al [189], a divalent copper-oxo cluster forming one extra framework μ-oxo bridge attached to two zeolite frameworks Al [189], a divalent copper-oxo cluster forming two extra framework μ-oxo bridges attached to two zeolite frameworks Al [188], and a divalent copper-oxo cluster forming three extra framework μ-oxo bridges attached to two zeolite frameworks Al [187,190,191].

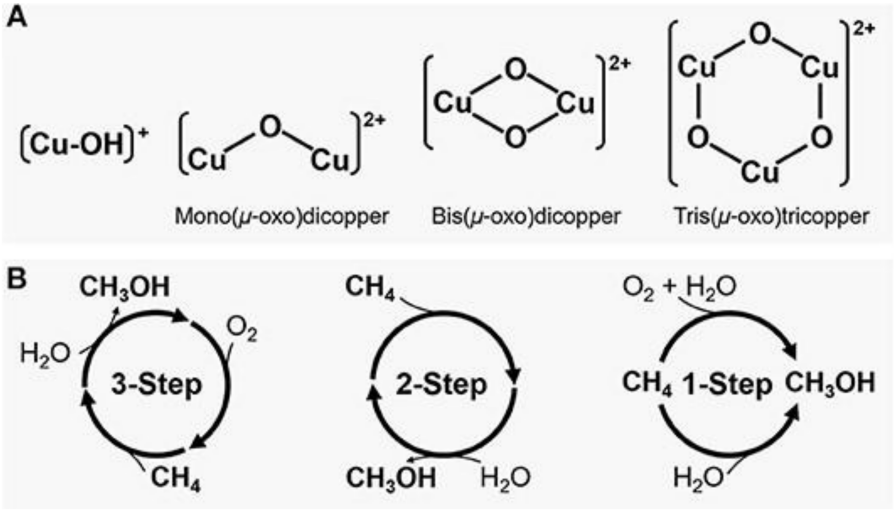

Figure 11. (**A**) Various proposed copper active species formed inside the zeolite pores and (**B**) Schemes for direct methane oxidation to methanol [187]. Copyright 2019, with permission from Frontiers.

Groothaert et al. [192] reported that Cu-ZSM-5 could be directly reacted with methane by pretreating it in an oxygen atmosphere, realizing methanol production without contact between methane and oxygen. The bis(μ-oxo) dicopper core detected by UV-vis spectroscopy, characterized by an intense band at 22,700 cm^{-1}, was proposed as the active site [188]. Woertink et al. [193] presented a bent mono-(μ-oxo) dicupric site in Cu-ZSM-5 based on DFT and normal coordinate analysis calculations. Interestingly, Li et al. [194] proposed that trinuclear copper-oxo clusters are highly reactive for the activation of C-H bonds in methane and their subsequent conversion to methanol. Moreover, similar trinuclear Cu-oxo clusters were found in the Cu-MOR for partial methane oxidation [195]. Vanelderen et al. [196] identified two distinct $[Cu\text{-}O\text{-}Cu]^{2+}$ sites in the Cu-MOR that are responsible for methane conversion. Mordenite micropores have been proven to provide a confined environment for highly stabilized trinuclear copper-oxo clusters [195]. The substitution of the weak oxidant N_2O for O_2 can convert 94% of the inactive Cu-O species into active Cu, and the methanol yield at 873 K is 1.5 times that of the O_2 atmosphere [197]. Ipek et al. [198] reported that the methanol generation rate over Cu-SSZ-15 in an N_2O atmosphere was more than twice that of Cu-mordenite and more than four times that of Cu-ZSM-5. The promoter also affects the performance of the Cu zeolite catalysts. Tomkins et al. [199] reported that Pt- and Pd-doped Cu-MOR catalysts exhibited higher reactivity under isothermal conditions (e.g., 200 °C) than after high-temperature activation, which is contrast to traditional Cu-zeolites. This was attributed to the aggregation of Pt and Pd precursors and Cu species to form bimetallic Cu clusters, facilitating the reduction of Cu oxides. Cu-SiO_2 has been reported to directly convert methane to methanol in a stepwise manner [200]. Although it can achieve the same methanol yield at 1073 K as Cu-MOR and Cu-ZSM-5 catalysts at 673 K, the results of this study contradict the previous view that reactive copper-oxygen species can only be generated on zeolites. Moreover, other active copper species or reaction mechanisms for the direct conversion of methane to methanol via the partial oxidation of methane over metal-containing zeolite catalysts have also been proposed [190,201,202].

Figure 11B shows the multistep processes in which Cu-based catalysts are first oxidized with O_2 at high temperatures, which are in contact with methane to form a methanol precursor adsorbed onto the active sites, and methanol can be extracted with H_2O to increase the methanol selectivity by separating the oxidation and methanol extraction steps. Even though optimum temperatures at each step vary according to the activation barrier for each reaction, from a practical point of view, a continuous process can be made without much difficulty [203]. These multi-step processes can be simplified by sacrificing the methanol yield, and finally, continuous one-step methanol synthesis from methane,

oxygen, and steam can be achieved by adjusting the reaction temperature and oxygen concentration [166,186,193]. Some catalytic activity data for the methane-to-methanol process are presented in Table 3. It is interesting that the active Cu species can be formed at much higher temperatures than that of the synthesis of the methoxy group and its desorption as methanol through hydrolysis. This is closely related to the fact that adsorbed water can be removed and active Cu species can be generated with oxygen only at high temperatures. The low fraction of active Cu species, which is responsible for the low methanol yield per total Cu, should be overcome in catalyst design.

Table 3. Summary of catalysts and their catalytic activity for gas-phase multi-step conversion of methane into methanol.

Catalysts				Pretreatment (gas/P/T/t)	Reaction (gas/P/T/t)	Methanol Extraction (gas/P/T/t)	Methanol Yield		Ref.
Name	Active Metal (Me) Loading (Wt%)	Me/Al	Si/Al				$mmol/g_{cat}$	$mmol/mol_{Cu}$	
Cu-ZSM-5 (MFI)	4.0	0.58	12	O_2/1 bar/500 °C	CH_4/1 bar/200 °C/0.25 h	Liquid water/1 bar/RT/1 h	8.2	13.1	[192]
Cu-mordenite (MOR)	4.3	0.4	11	O_2/1 bar/400 °C/4 h	CH_4/1 bar/200 °C/0.33 h	Steam in He/1 bar/RT/2 h	13	19.3	[204]
Cu-mordenite (MOR)	/	0.4	6.5	He/1 bar/400 °C/1 h	CH_4/7 bar/200 °C/0.5 h	2.4% steam in He/1 bar/200 °C/2–4 h	/	204	[205]
Cu-mordenite (MOR)	/	0.6	46	O_2/1 bar/400 °C/1 h	CH_4/7 bar/200 °C/0.5 h	2.4% steam in He/1 bar/200 °C/2–4 h	/	316	[206]
Cu-mordenite (MOR)	2.0	0.4	20	10% N_2O/1 bar/600 °C/2 h	CH_4/1 bar/150 °C/1 h	7% steam in N_2/1 bar/135 °C	97	310	[197]
Cu-mordenite (MOR)	2.0	0.4	20	O_2/1 bar/450 °C/2 h	CH_4/1 bar/150 °C/1 h	7% steam in N_2/1 bar/135 °C	67	214	[197]
Cu-mordenite (MOR)	4.1	0.38	8.5	O_2/1 bar/450 °C/4 h	5% CH_4/1 bar/200 °C/0.5 h	Liquid water/1 bar/25 °C/2 h	19	29.7	[134]
Cu-mordenite (MOR)	2.3	0.18	7	O_2/1 bar/500 °C/8 h	CH_4/1 bar/200 °C/6 h	10% steam/1 bar/200 °C/1 h	169	470	[207]
Cu-SSZ-13 (CHA)	3.9	0.5	5	O_2/1 bar/500 °C/2 h	CH_4/1 bar/200 °C/1 h	10% steam/1 bar/200 °C/2 h	125	200	[208]
Cu-ZSM-5 (MFI)	3.3	0.5	17	O_2/1 bar/450 °C/1 h	CH_4/1 bar/200 °C/8 h	Steam/1 bar/135 °C/2 h	89	172	[209]
Cu-mordenite (MOR)	2.2	0.28	10	O_2/1 bar/450 °C/2 h	CH_4/35 bar/200 °C/20 h	Steam/1 bar/200 °C/2 h	/	390	[210]
Cu-SSZ-13 (CHA)	2.2	0.25	11	He/1 bar/400 °C/0.5 h	CH_4/1 bar/200 °C/5 h	3.2% steam in He/1 bar/200 °C	60	174	[211]
Cu-SSZ-13 (CHA)	2.0	0.22	10	He/1 bar/400 °C/0.5 h	CH_4/1 bar/200 °C/15 h	3.2% steam in He/1 bar/200 °C	25	76.3	[212]
Cu-SUZ-4 (SZR)	4.3	0.43	8.2	O_2/1 bar/450 °C/4 h	CH_4/1 bar/200 °C/0.5 h	Liquid water/1 bar/RT/2 h	14.4	11.5	[213]

Table 3. *Cont.*

Catalysts				Pretreatment (gas/P/T/t)	Reaction (gas/P/T/t)	Methanol Extraction (gas/P/T/t)	Methanol Yield		Ref.
Name	Active Metal (Me) Loading (Wt%)	Me/Al	Si/Al				$mmol/g_{cat}$	$mmol/mol_{Cu}$	
Cu-omega (MAZ)	5.9	0.29	3.2	O_2/1 bar/ 450 °C/4 h	CH_4/1 bar/ 200 °C/0.5 h	Liquid water/1 bar/ RT/2 h	86.1	92.6	[213]
Cu-UZM-22 (MEI)	4.3	0.32	4.8	O_2/1 bar/ 550 °C/4 h	CH_4/1 bar/ 200 °C/0.5 h	Liquid water/1 bar/ RT/2 h	16.1	23.8	[213]
Cu-omega (MAZ)	4.64	/	4.0	O_2/1 bar/ 450 °C/4 h	CH_4/6 bar/ 200 °C/0.5 h	Liquid water/1 bar/ RT/2 h	144.8	210	[214]
Cu-mordenite (MOR)	1.8	/	9.3	O_2/1 bar/ 500 °C/1 h	CH_4/1 bar/ 200 °C/4 h	50% Steam/1 bar/ 135 °C	160	565	[215]
Cu-ZSM-5 (MFI)	2.5	0.37	11.5	O_2/1 bar/ 550 °C/0.5 h	CH_4/1 bar/ 210 °C/0.5 h	$H_2O + O_2 + CH_4$/1 bar/ 210 °C/0.5 h	82	210	[169]
Cu-SSZ-13 (CHA)	3.2	0.4	12	O_2/1 bar/ 450 °C/2 h	CH_4/1 bar/ 200 °C/1 h	Steam/1 bar/ 200°C/1 h	45	90	[198]
Cu-SSZ-13 (CHA)	3.2	0.4	12	N_2O/1 bar/ 450 °C/2 h	CH_4/1 bar/ 200 °C/1 h	Steam/1 bar/ 200°C/1 h	35	70	[198]
Ni-ZSM-5 (MFI)	5.0	0.1	15	O_2/1 bar/ 550 °C/3 h	CH_4/1 bar/ 175 °C/0.75 h	Liquid water/1 bar/ RT/24 h	5.8	6.9	[216]
Ni-ferrierite (FER)	1.0	0.1	8.6	Ar/1 bar/ 450 °C/3 h—O_2/1 bar/ RT/1 h	CH_4/1 bar/ RT	/	116	680	[217]
Cu@UiO-bpy	19.2	/	/	O_2/1 bar/ 200 °C/3 h	CH_4/1 bar/ 200 °C/3 h	Steam with He/1 bar	24.3	8.1	[218]
Fe-SSZ-13 (CHA)	2.7	0.43	13	He/1 bar/ 900 °C/5 h—N_2O/1 bar/ 180 °C/0.42 h	CH_4/1 bar/ RT/0.17 h	Steam with He/1bar/ RT/25 h	134	270	[179]

Recently, the anaerobic oxidation of methane into methanol has also been reported by several groups [155,205]. Because steam is used as an oxidant in this case, it is not thermodynamically favorable (Equation (7)) compared to the aerobic oxidation of methane, especially at lower temperatures. However, the coproduction of hydrogen is advantageous for the anaerobic oxidation of methane.

$$CH_4(g) + H_2O(g) \rightarrow CH_3OH(g) + H_2(g)\ \Delta G^o_{298K} = 117\ kJ/mol,\ \Delta H^0_{298K} = 116\ kJ/mol \quad (7)$$

4. Conclusions and Outlook

Methane is a clean and abundant resource; therefore, its usage only as fuel is not plausible. Although methane is also currently utilized as a chemical feedstock via indirect energy-intensive pathways, the development of direct methane conversion technologies can pave the way for the active utilization of methane found in various small-scale natural gas resources. The selective oxidation of methane is a promising candidate for direct methane conversion from a thermodynamic perspective. The major hurdle for its commercialization is catching two rabbits simultaneously, that is, high methane conversion and product

selectivity should be achieved simultaneously. Therefore, novel catalysts and processes must be developed. In this review, we assessed some catalysts for two typical reactions (methane-to-formaldehyde and methane-to-methanol).

The active catalysts for the gas-phase selective oxidation of methane into formaldehyde have highly dispersed, isolated active species that are responsible for the high formaldehyde selectivity but low methane conversion. At present, the commercial operation of this system is far flung. In addition, the structure of the active site and reaction mechanism have not been sufficiently resolved. Recent developments in computational chemistry will be helpful in understanding the detailed reaction mechanism of active site for each catalyst. Based on these results, well-defined active catalysts can be designed and prepared by considering various factors such as promoters, loadings, supports, and catalyst precursors.

Similar scientific issues have been confronted with the gas-phase selective oxidation of methane into methanol. A high methanol selectivity can only be achieved at low methane conversion levels. Although there are numerous studies on the gas-phase oxidation of methane into methanol over heterogeneous catalysts, including the incorporation of transitional metals into zeolites mimicking the MMO structure, the catalytic performance still does not meet the requirements for commercialization. Although Fe-zeolites exhibit comparatively meaningful performance with N_2O as an oxidant, N_2O is not an ideal oxidant for environmental and economic reasons. The direct use of oxygen as an oxidant is a critical advantage of Cu-based catalysts for direct methanol synthesis from methane under milder conditions. However, the methanol productivity is still much lower than that of commercial methanol synthesis processes [219].

It appears there is a limitation to the gas-phase partial oxidation of methane into methane oxygenates. What about the liquid-phase selective oxidation of methane? It bypasses this difficulty by using protecting groups against over-oxidation of methane. Methyl bisulfate and methyl trifluoroacetate are stable methanol precursors in sulfuric acid and trifluoroacetic acid, respectively. This concept cannot be directly applied to gas-phase partial oxidation of methane. However, other engineering concepts, including a membrane reactor in which the concentration of oxygen in the reactor can be controlled to be low so as not to cause overoxidation, can be proposed and examined. The separation between methane oxidation and product recovery was also proposed but not much successful in achieving high productivity of methane oxygenates. To date, we have focused on the development of active catalysts in terms of methane conversion and product selectivity, which are not the only factors determining the economic feasibility of this direct methane conversion process. The approach from the overall process system, including the reactor and separation units, can provide other reaction conditions where new catalysts are more plausible than the conventional catalysts reported previously.

Author Contributions: Conceptualization, E.D.P.; writing—original draft preparation, Z.C.X.; writing—review and editing, E.D.P.; supervision, project administration, and funding acquisition, E.D.P. All authors have read and agreed to the published version of the manuscript.

Funding: This work was supported by the C1 Gas Refinery Program through the National Research Foundation of Korea (NRF), funded by the Ministry of Science, ICT, and Future Planning (2015M3D3A1A01064899).

Conflicts of Interest: The authors declare no conflict of interest.

References

1. Olah, G.A. Beyond Oil and Gas: The Methanol Economy. *Angew. Chem. Int. Ed.* **2005**, *44*, 2636–2639. [CrossRef] [PubMed]
2. Tiwary, R.K. Environmental Impact of Coal Mining on Water Regime and Its Management. *Water Air Soil Pollut.* **2001**, *132*, 185–199. [CrossRef]
3. NaturalGas.Org. Available online: http://naturalgas.org/overview/background/ (accessed on 14 February 2022).
4. BP Statistical Review of World Energy Globally Consistent Data on World Energy Markets and Authoritative Publications in the Field of Energy. *BP Energy Outlook* **2021**, *70*, 8–20.
5. Schwach, P.; Pan, X.; Bao, X. Direct Conversion of Methane to Value-Added Chemicals over Heterogeneous Catalysts: Challenges and Prospects. *Chem. Rev.* **2017**, *117*, 8497–8520. [CrossRef] [PubMed]

6. Kerr, R.A. Natural Gas From Shale Bursts Onto the Scene. *Science* **2010**, *328*, 1624–1626. [CrossRef]
7. Dry, M.E. The Fischer-Tropsch Process: 1950–2000. *Catal. Today* **2002**, *71*, 227–241. [CrossRef]
8. Schulz, H. Short History and Present Trends of Fischer–Tropsch Synthesis. *Appl. Catal. A Gen.* **1999**, *186*, 3–12. [CrossRef]
9. Cheng, K.; Kang, J.; King, D.L.; Subramanian, V.; Zhou, C.; Zhang, Q.; Wang, Y. *Advances in Catalysis for Syngas Conversion to Hydrocarbons*; Song, C.B.T.-A., Ed.; Academic Press: Cambridge, MA, USA, 2017; Volume 60, pp. 125–208.
10. Holmen, A. Direct Conversion of Methane to Fuels and Chemicals. *Catal. Today* **2009**, *142*, 2–8. [CrossRef]
11. Guo, Z.; Liu, B.; Zhang, Q.; Deng, W.; Wang, Y.; Yang, Y. Recent Advances in Heterogeneous Selective Oxidation Catalysis for Sustainable Chemistry. *Chem. Soc. Rev.* **2014**, *43*, 3480. [CrossRef]
12. Otsuka, K.; Wang, Y. Direct Conversion of Methane into Oxygenates. *Appl. Catal. A Gen.* **2001**, *222*, 145–161. [CrossRef]
13. Spivey, J.J.; Hutchings, G. Catalytic Aromatization of Methane. *Chem. Soc. Rev.* **2014**, *43*, 792–803. [CrossRef] [PubMed]
14. Kondratenko, E.v.; Peppel, T.; Seeburg, D.; Kondratenko, V.A.; Kalevaru, N.; Martin, A.; Wohlrab, S. Methane Conversion into Different Hydrocarbons or Oxygenates: Current Status and Future Perspectives in Catalyst Development and Reactor Operation. *Catal. Sci. Technol.* **2017**, *7*, 366–381. [CrossRef]
15. Tang, P.; Zhu, Q.; Wu, Z.; Ma, D. Methane Activation: The Past and Future. *Energy Environ. Sci.* **2014**, *7*, 2580–2591. [CrossRef]
16. Alvarez-Galvan, M.C.; Mota, N.; Ojeda, M.; Rojas, S.; Navarro, R.M.; Fierro, J.L.G. Direct Methane Conversion Routes to Chemicals and Fuels. *Catal. Today* **2011**, *171*, 15–23. [CrossRef]
17. Zavyalova, U.; Holena, M.; Schlögl, R.; Baerns, M. Statistical Analysis of Past Catalytic Data on Oxidative Methane Coupling for New Insights into the Composition of High-Performance Catalysts. *ChemCatChem* **2011**, *3*, 1935–1947. [CrossRef]
18. Gunsalus, N.J.; Koppaka, A.; Park, S.H.; Bischof, S.M.; Hashiguchi, B.G.; Periana, R.A. Homogeneous Functionalization of Methane. *Chem. Rev.* **2017**, *117*, 8521–8573. [CrossRef]
19. Ravi, M.; Ranocchiari, M.; van Bokhoven, J.A. The Direct Catalytic Oxidation of Methane to Methanol-A Critical Assessment. *Angew. Chem. Int. Ed.* **2017**, *56*, 16464–16483. [CrossRef]
20. De Vekki, A.v.; Marakaev, S.T. Catalytic Partial Oxidation of Methane to Formaldehyde. *Russ. J. Appl. Chem.* **2009**, *82*, 521–536. [CrossRef]
21. Olivos-Suarez, A.I.; Szécsényi, À.; Hensen, E.J.M.; Ruiz-Martinez, J.; Pidko, E.A.; Gascon, J. Strategies for the Direct Catalytic Valorization of Methane Using Heterogeneous Catalysis: Challenges and Opportunities. *ACS Catal.* **2016**, *6*, 2965–2981. [CrossRef]
22. Sirajuddin, S.; Rosenzweig, A.C. Enzymatic Oxidation of Methane. *Biochemistry* **2015**, *54*, 2283–2294. [CrossRef]
23. Gol'Dshleger, N.F.; Es' Kova, V.v.; Shilov, A.E.; Shteinman, A.A. Reactions of Alkanes in Solutions of Platinum Chloride Complexes. *Zhurnal Fiz. Khimi* **1972**, *46*, 1353–1354.
24. Periana, R.A.; Taube, D.J.; Evitt, E.R.; Löffler, D.G.; Wentrcek, P.R.; Voss, G.; Masuda, T. A Mercury-Catalyzed, High-Yield System for the Oxidation of Methane to Methanol. *Science* **1993**, *259*, 340–343. [CrossRef]
25. Periana, R.A.; Taube, D.J.; Gamble, S.; Taube, H.; Satoh, T.; Fujii, H. Platinum Catalysts for the High-Yield Oxidation of Methane to a Methanol Derivative. *Science* **1998**, *280*, 560–564. [CrossRef] [PubMed]
26. Mukhopadhyay, S.; Zerella, M.; Bell, A.T. A High-Yield, Liquid-Phase Approach for the Partial Oxidation of Methane to Methanol Using SO_3 as the Oxidant. *Adv. Synth. Catal.* **2005**, *347*, 1203–1206. [CrossRef]
27. Newton, M.A.; Knorpp, A.J.; Sushkevich, V.L.; Palagin, D.; van Bokhoven, J.A. Active Sites and Mechanisms in the Direct Conversion of Methane to Methanol Using Cu in Zeolitic Hosts: A Critical Examination. *Chem. Soc. Rev.* **2020**, *49*, 1449–1486. [CrossRef]
28. Sen, A.; Benvenuto, M.A.; Lin, M.; Hutson, A.C.; Basickes, N. Activation of Methane and Ethane and Their Selective Oxidation to the Alcohols in Protic Media. *J. Am. Chem. Soc.* **1994**, *116*, 998–1003. [CrossRef]
29. Hashiguchi, B.G.; Bischof, S.M.; Konnick, M.M.; Periana, R.A. Designing Catalysts for Functionalization of Unactivated C–H Bonds Based on the CH Activation Reaction. *Acc. Chem. Res.* **2012**, *45*, 885–898. [CrossRef]
30. Ohyama, J.; Hirayama, A.; Kondou, N.; Yoshida, H.; Machida, M.; Nishimura, S.; Hirai, K.; Miyazato, I.; Takahashi, K. Data Science Assisted Investigation of Catalytically Active Copper Hydrate in Zeolites for Direct Oxidation of Methane to Methanol Using H_2O_2. *Sci. Rep.* **2021**, *11*, 2067. [CrossRef]
31. Sun, L.; Wang, Y.; Guan, N.; Li, L. Methane Activation and Utilization: Current Status and Future Challenges. *Energy Technol.* **2020**, *8*, 1900826. [CrossRef]
32. Wang, X.; Wang, Y.; Tang, Q.; Guo, Q.; Zhang, Q.; Wan, H. MCM-41-Supported Iron Phosphate Catalyst for Partial Oxidation of Methane to Oxygenates with Oxygen and Nitrous Oxide. *J. Catal.* **2003**, *217*, 457–467. [CrossRef]
33. Zhang, Q.; Li, Y.; An, D.; Wang, Y. Catalytic Behavior and Kinetic Features of FeO_x/SBA-15 Catalyst for Selective Oxidation of Methane by Oxygen. *Appl. Catal. A Gen.* **2009**, *356*, 103–111. [CrossRef]
34. Arena, F.; Gatti, G.; Martra, G.; Coluccia, S.; Stievano, L.; Spadaro, L.; Famulari, P.; Parmaliana, A. Structure and Reactivity in the Selective Oxidation of Methane to Formaldehyde of Low-Loaded FeO_x/SiO_2 Catalysts. *J. Catal.* **2005**, *231*, 365–380. [CrossRef]
35. Li, Y.; An, D.; Zhang, Q.; Wang, Y. Copper-Catalyzed Selective Oxidation of Methane by Oxygen: Studies on Catalytic Behavior and Functioning Mechanism of CuO_x/SBA-15. *J. Phys. Chem. C* **2008**, *112*, 13700–13708. [CrossRef]
36. Tian, J.; Tan, J.; Zhang, Z.; Han, P.; Yin, M.; Wan, S.; Lin, J.; Wang, S.; Wang, Y. Direct Conversion of Methane to Formaldehyde and CO on B_2O_3 Catalysts. *Nat. Commun.* **2020**, *11*, 5693. [CrossRef]
37. Moro-Oka, Y.; Ueda, W. Multicomponent Bismuth Molybdate Catalyst: A Highly Functionalized Catalyst System for the Selective Oxidation of Olefin. *Adv. Catal.* **1994**, *40*, 233–273. [CrossRef]

38. Mars, P.; van Krevelen, D.W. Oxidations Carried out by Means of Vanadium Oxide Catalysts. *Chem. Eng. Sci.* **1954**, *3*, 41–59. [CrossRef]
39. Schlögl, R.; Knop-Gericke, A.; Hävecker, M.; Wild, U.; Frickel, D.; Ressler, T.; Jentoft, R.E.; Wienold, J.; Mestl, G.; Blume, A.; et al. In Situ Analysis of Metal-Oxide Systems Used for Selective Oxidation Catalysis: How Essential Is Chemical Complexity? *Top. Catal.* **2001**, *15*, 219–228. [CrossRef]
40. Grasselli, R.K. Fundamental Principles of Selective Heterogeneous Oxidation Catalysis. *Top. Catal.* **2002**, *21*, 79–88. [CrossRef]
41. Grasselli, R.K. Advances and Future Trends in Selective Oxidation and Ammoxidation Catalysis. *Catal. Today* **1999**, *49*, 141–153. [CrossRef]
42. Haber, J.; Turek, W. Kinetic Studies as a Method to Differentiate between Oxygen Species Involved in the Oxidation of Propene. *J. Catal.* **2000**, *190*, 320–326. [CrossRef]
43. Ohler, N.; Bell, A.T. Study of the Elementary Processes Involved in the Selective Oxidation of Methane over MoO_x/SiO_2. *J. Phys. Chem. B* **2006**, *110*, 2700–2709. [CrossRef] [PubMed]
44. Ohler, N.; Bell, A.T. Selective Oxidation of Methane over MoO_x/SiO_2: Isolation of the Kinetics of Reactions Occurring in the Gas Phase and on the Surfaces of SiO_2 and MoO_x. *J. Catal.* **2005**, *231*, 115–130. [CrossRef]
45. Baldwin, T.R.; Burch, R.; Squire, G.D.; Tsang, S.C. Influence of Homogeneous Gas Phase Reactions in the Partial Oxidation of Methane to Methanol and Formaldehyde in the Presence of Oxide Catalysts. *Appl. Catal.* **1991**, *74*, 137–152. [CrossRef]
46. Ohler, N.; Bell, A.T. A Study of the Redox Properties of MoO_x/SiO_2. *J. Phys. Chem. B* **2005**, *109*, 23419–23429. [CrossRef] [PubMed]
47. Chempath, S.; Bell, A.T. A DFT Study of the Mechanism and Kinetics of Methane Oxidation to Formaldehyde Occurring on Silica-Supported Molybdena. *J. Catal.* **2007**, *247*, 119–126. [CrossRef]
48. Lee, E.L.; Wachs, I.E. In Situ Raman Spectroscopy of SiO_2-Supported Transition Metal Oxide Catalysts: An Isotopic ^{18}O-^{16}O Exchange Study. *J. Phys. Chem. C* **2008**, *112*, 6487–6498. [CrossRef]
49. Lee, E.L.; Wachs, I.E. In Situ Spectroscopic Investigation of the Molecular and Electronic Structures of SiO_2 Supported Surface Metal Oxides. *J. Phys. Chem. C* **2007**, *111*, 14410–14425. [CrossRef]
50. Handzlik, J.; Ogonowski, J. Structure of Isolated Molybdenum(VI) and Molybdenum(IV) Oxide Species on Silica: Periodic and Cluster DFT Studies. *J. Phys. Chem. C* **2012**, *116*, 5571–5584. [CrossRef]
51. Tian, H.; Roberts, C.A.; Wachs, I.E. Molecular Structural Determination of Molybdena in Different Environments: Aqueous Solutions, Bulk Mixed Oxides, and Supported MoO_3 Catalysts. *J. Phys. Chem. C* **2010**, *114*, 14110–14120. [CrossRef]
52. Shimura, K.; Fujitani, T. Effects of Promoters on the Performance of a VO/SiO_2 Catalyst for the Oxidation of Methane to Formaldehyde. *Appl. Catal. A Gen.* **2019**, *577*, 44–51. [CrossRef]
53. Erdőhelyi, A.; Németh, R.; Hancz, A.; Oszkó, A. Partial Oxidation of Methane on Potassium-Promoted WO_3/SiO_2 and on K_2WO_4/SiO_2 Catalysts. *Appl. Catal. A Gen.* **2001**, *211*, 109–121. [CrossRef]
54. Hargreaves, J.S.J.; Hutchings, G.J.; Joyner, R.W. Control of Product Selectivity in the Partial Oxidation of Methane. *Nature* **1990**, *348*, 428–429. [CrossRef]
55. Aoki, K.; Ohmae, M.; Nanba, T.; Takeishi, K.; Azuma, N.; Ueno, A.; Ohfune, H.; Hayashi, H.; Udagawa, Y. Direct Conversion of Methane into Methanol over MoO_3/SiO_2 Catalyst in an Excess Amount of Water Vapor. *Catal. Today* **1998**, *45*, 29–33. [CrossRef]
56. Kim, Y.; Kim, T.Y.; Song, C.K.; Lee, K.R.; Bae, S.; Park, H.; Yun, D.; Yun, Y.S.; Nam, I.; Park, J.; et al. Redox-Driven Restructuring of Lithium Molybdenum Oxide Nanoclusters Boosts the Selective Oxidation of Methane. *Nano Energy* **2021**, *82*, 105704. [CrossRef]
57. Chen, P.; Xie, Z.; Zhao, Z.; Li, J.; Liu, B.; Liu, B.; Fan, X.; Kong, L.; Xiao, X. Study on the Selective Oxidation of Methane over Highly Dispersed Molybdenum-Incorporated KIT-6 Catalysts. *Catal. Sci. Technol.* **2021**, *11*, 4083–4097. [CrossRef]
58. Lou, Y.; Tang, Q.; Wang, H.; Chia, B.; Wang, Y.; Yang, Y. Selective Oxidation of Methane to Formaldehyde by Oxygen over SBA-15-Supported Molybdenum Oxides. *Appl. Catal. A Gen.* **2008**, *350*, 118–125. [CrossRef]
59. Pei, S.; Yue, B.; Qian, L.; Yan, S.; Cheng, J.; Zhou, Y.; Xie, S.; He, H. Preparation and Characterization of P–Mo–V Mixed Oxide-Incorporating Mesoporous Silica Catalysts for Selective Oxidation of Methane to Formaldehyde. *Appl. Catal. A Gen.* **2007**, *329*, 148–155. [CrossRef]
60. Zhang, X.; He, D.H.; Zhang, Q.J.; Ye, Q.; Xu, B.Q.; Zhu, Q.M. Selective Oxidation of Methane to Formaldehyde over Mo/ZrO_2 Catalysts. *Appl. Catal. A Gen.* **2003**, *249*, 107–117. [CrossRef]
61. Akiyama, T.; Sei, R.; Takenaka, S. Partial Oxidation of Methane to Formaldehyde over Copper–Molybdenum Complex Oxide Catalysts. *Catal. Sci. Technol.* **2021**, *11*, 5273–5281. [CrossRef]
62. Dai, L.X.; Teng, Y.H.; Tabata, K.; Suzuki, E.; Tatsumi, T. Catalytic Application of Mo-Incorporated SBA-1 Mesoporous Molecular Sieves to Partial Oxidation of Methane. *Microporous Mesoporous Mater.* **2001**, *44–45*, 573–580. [CrossRef]
63. Yang, W.; Wang, X.; Guo, Q.; Zhang, Q.; Wang, Y. Superior Catalytic Performance of Phosphorus-Modified Molybdenum Oxide Clusters Encapsulated inside SBA-15 in the Partial Oxidation of Methane. *New J. Chem.* **2003**, *27*, 1301. [CrossRef]
64. Erdohelyi, A.; Fodor, K.; Solymosi, F. Partial Oxidation of Methane on Supported Potassium Molybdate. *J. Catal.* **1997**, *166*, 244–253. [CrossRef]
65. Kastanas, G.N.; Tsigdinos, G.A.; Schwank, J. Selective Oxidation of Methane over Vycor Glass, Quartz Glass and Various Silica, Magnesia and Alumina Surfaces. *Appl. Catal.* **1988**, *44*, 33–51. [CrossRef]
66. Yang, E.; Lee, J.G.; Park, E.D.; An, K. Methane Oxidation to Formaldehyde over Vanadium Oxide Supported on Various Mesoporous Silicas. *Korean J. Chem. Eng.* **2021**, *38*, 1224–1230. [CrossRef]

67. Yang, E.; Lee, J.G.; Kim, D.H.; Jung, Y.S.; Kwak, J.H.; Park, E.D.; An, K. SiO_2@V_2O_5@Al_2O_3 Core–Shell Catalysts with High Activity and Stability for Methane Oxidation to Formaldehyde. *J. Catal.* **2018**, *368*, 134–144. [CrossRef]
68. Kunkel, B.; Wohlrab, S. Enhancement and Limits of the Selective Oxidation of Methane to Formaldehyde over V-SBA-15: Influence of Water Cofeed and Product Decomposition. *Catal. Commun.* **2021**, *155*, 106317. [CrossRef]
69. Volpe, M.A. Partial Oxidation of Methane over VO_x/α-Al_2O_3 Catalysts. *Appl. Catal. A Gen.* **2001**, *210*, 355–361. [CrossRef]
70. Berndt, H.; Martin, A.; Brückner, A.; Schreier, E.; Müller, D.; Kosslick, H.; Wolf, G.U.; Lücke, B. Structure and Catalytic Properties of VO_x/MCM Materials for the Partial Oxidation of Methane to Formaldehyde. *J. Catal.* **2000**, *191*, 384–400. [CrossRef]
71. Matsuda, A.; Tateno, H.; Kamata, K.; Hara, M. Iron Phosphate Nanoparticle Catalyst for Direct Oxidation of Methane into Formaldehyde: Effect of Surface Redox and Acid–Base Properties. *Catal. Sci. Technol.* **2021**, *11*, 6987–6998. [CrossRef]
72. Zhang, H.; Sun, K.; Feng, Z.; Ying, P.; Li, C. Studies on the SbO_x Species of SbO_x/SiO_2 Catalysts for Methane-Selective Oxidation to Formaldehyde. *Appl. Catal. A Gen.* **2006**, *305*, 110–119. [CrossRef]
73. Ohyama, J.; Abe, D.; Hirayama, A.; Iwai, H.; Tsuchimura, Y.; Sakamoto, K.; Irikura, M.; Nakamura, Y.; Yoshida, H.; Machida, M.; et al. Selective Oxidation of Methane to Formaldehyde over a Silica-Supported Cobalt Single-Atom Catalyst. *J. Phys. Chem. C* **2022**, *126*, 1785–1792. [CrossRef]
74. Foster, N.R. Direct Catalytic Oxidation of Methane to Methanol—A Review. *Appl. Catal.* **1985**, *19*, 1–11. [CrossRef]
75. Banares, M.A.; Fierro, J.L.G.; Moffat, J.B. The Partial Oxidation of Methane on MoO_3/SiO_2 Catalysts: Influence of the Molybdenum Content and Type of Oxidant. *J. Catal.* **1993**, *142*, 406–417. [CrossRef]
76. Spencer, N. Partial Oxidation of Methane to Formaldehyde by Means of Molecular Oxygen. *J. Catal.* **1988**, *109*, 187–197. [CrossRef]
77. Barbaux, Y.; Elamrani, A.R.; Payen, E.; Gengembre, L.; Bonnelle, J.P.; Grzybowska, B. Silica Supported Molybdena Catalysts. *Appl. Catal.* **1988**, *44*, 117–132. [CrossRef]
78. Liu, H.F.; Liu, R.S.; Liew, K.Y.; Johnson, R.E.; Lunsford, J.H. Partial Oxidation of Methane by Nitrous Oxide over Molybdenum on Silica. *J. Am. Chem. Soc.* **1984**, *106*, 4117–4121. [CrossRef]
79. Plyuto, Y.V.; Babich, I.V.; Plyuto, I.V.; van Langeveld, A.D.; Moulijn, J.A. XPS Studies of MoO_3/Al_2O_3 and MoO_3/SiO_2 Systems. *Appl. Surf. Sci.* **1997**, *119*, 11–18. [CrossRef]
80. Thomas, D.J.; Willi, R.; Baiker, A. Partial Oxidation of Methane: The Role of Surface Reactions. *Ind. Eng. Chem. Res.* **1992**, *31*, 2272–2278. [CrossRef]
81. Liu, Y.M.; Cao, Y.; Yi, N.; Feng, W.L.; Dai, W.L.; Yan, S.R.; He, H.Y.; Fan, K.N. Vanadium Oxide Supported on Mesoporous SBA-15 as Highly Selective Catalysts in the Oxidative Dehydrogenation of Propane. *J. Catal.* **2004**, *224*, 417–428. [CrossRef]
82. Nieminen, V.; Kumar, N.; Salmi, T.; Murzin, D.Y. N-Butane Isomerization over Pt–H–MCM-41. *Catal. Commun.* **2004**, *5*, 15–19. [CrossRef]
83. Solsona, B.; Blasco, T.; López Nieto, J.M.; Peña, M.L.; Rey, F.; Vidal-Moya, A. Vanadium Oxide Supported on Mesoporous MCM-41 as Selective Catalysts in the Oxidative Dehydrogenation of Alkanes. *J. Catal.* **2001**, *203*, 443–452. [CrossRef]
84. Fornés, V.; López, C.; López, H.H.; Martínez, A. Catalytic Performance of Mesoporous VO_x/SBA-15 Catalysts for the Partial Oxidation of Methane to Formaldehyde. *Appl. Catal. A Gen.* **2003**, *249*, 345–354. [CrossRef]
85. Chen, K.; Xie, S.; Bell, A.T.; Iglesia, E. Alkali Effects on Molybdenum Oxide Catalysts for the Oxidative Dehydrogenation of Propane. *J. Catal.* **2000**, *195*, 244–252. [CrossRef]
86. Zhao, Z.; Liu, J.; Duan, A.; Xu, C.; Kobayashi, T.; Wachs, I.E. Effects of Alkali Metal Cations on the Structures, Physico-Chemical Properties and Catalytic Behaviors of Silica-Supported Vanadium Oxide Catalysts for the Selective Oxidation of Ethane and the Complete Oxidation of Diesel Soot. *Top. Catal.* **2006**, *38*, 309–325. [CrossRef]
87. Ivars, F.; Solsona, B.; Botella, P.; Soriano, M.D.; López Nieto, J.M. Selective Oxidation of Propane over Alkali-Doped Mo-V-Sb-O Catalysts. *Catal. Today* **2009**, *141*, 294–299. [CrossRef]
88. Grant, J.T.; Carrero, C.A.; Love, A.M.; Verel, R.; Hermans, I. Enhanced Two-Dimensional Dispersion of Group V Metal Oxides on Silica. *ACS Catal.* **2015**, *5*, 5787–5793. [CrossRef]
89. Teng, Y.; Kobayashi, T. Reaction Pathways for the Oxygenates Formation from Propane and Oxygen over Potassium-modified Fe/SiO_2 Catalysts. *Catal. Lett.* **1998**, *55*, 33–38. [CrossRef]
90. Wallis, P.; Schönborn, E.; Kalevaru, V.N.; Martin, A.; Wohlrab, S. Enhanced Formaldehyde Selectivity in Catalytic Methane Oxidation by Vanadia on Ti-Doped SBA-15. *RSC Adv.* **2015**, *5*, 69509–69513. [CrossRef]
91. Grzybowska, B.; Mekšs, P.; Grabowski, R.; Wcisto, K.; Barbaux, Y.; Gengembre, L. Effect of Potassium Addition to V_2O_5/TiO_2 and MoO_3/TiO_2 Catalysts on Their Physicochemical and Catalytic Properties in Oxidative Dehydrogenation of Propane. In *New Developments in Selective Oxidation II*; Corberán, V.C., Bellón, S.V.B.T.-S., Eds.; Elsevier: Amsterdam, The Netherlands, 1994; Volume 82, pp. 151–158.
92. Grzybowska-Świerkosz, B. Effect of Additives on the Physicochemical and Catalytic Properties of Oxide Catalysts in Selective Oxidation Reactions. *Top. Catal.* **2002**, *21*, 35–46. [CrossRef]
93. Deo, G.; Wachs, I.E. Reactivity of Supported Vanadium Oxide Catalysts: The Partial Oxidation of Methanol. *J. Catal.* **1994**, *146*, 323–334. [CrossRef]
94. Liu, Q.; Li, J.; Zhao, Z.; Gao, M.; Kong, L.; Liu, J.; Wei, Y. Synthesis, Characterization, and Catalytic Performances of Potassium-Modified Molybdenum-Incorporated KIT-6 Mesoporous Silica Catalysts for the Selective Oxidation of Propane to Acrolein. *J. Catal.* **2016**, *344*, 38–52. [CrossRef]

95. Verbruggen, N.F.D.; von Hippel, L.M.J.; Mestl, G.; Lengeler, B.; Knözinger, H. Structure of K-Doped Molybdena-on-Silica Catalysts As Studied by X-ray Absorption and Raman Spectroscopy. *Langmuir* **2002**, *10*, 3073–3080. [CrossRef]
96. Liu, J.; Yu, L.; Zhao, Z.; Chen, Y.; Zhu, P.; Wang, C.; Luo, Y.; Xu, C.; Duan, A.; Jiang, G. Potassium-Modified Molybdenum-Containing SBA-15 Catalysts for Highly Efficient Production of Acetaldehyde and Ethylene by the Selective Oxidation of Ethane. *J. Catal.* **2012**, *285*, 134–144. [CrossRef]
97. Millner, T.; Neugebauer, J. Volatility of the Oxides of Tungsten and Molybdenum in the Presence of Water Vapour. *Nature* **1949**, *163*, 601–602. [CrossRef]
98. Blasco, T.; Nieto, J.M.L. Oxidative Dyhydrogenation of Short Chain Alkanes on Supported Vanadium Oxide Catalysts. *Appl. Catal. A Gen.* **1997**, *157*, 117–142. [CrossRef]
99. Faraldos, M.; Bañares, M.A.; Anderson, J.A.; Hu, H.; Wachs, I.E.; Fierro, J.L.G. Comparison of Silica-Supported MoO_3 and V_2O_5 Catalysts in the Selective Partial Oxidation of Methane. *J. Catal.* **1996**, *160*, 214–221. [CrossRef]
100. Gao, X.; Jehng, J.M.; Wachs, I.E. In Situ UV-Vis-NIR Diffuse Reflectance and Raman Spectroscopic Studies of Propane Oxidation over ZrO_2-Supported Vanadium Oxide Catalysts. *J. Catal.* **2002**, *209*, 43–50. [CrossRef]
101. Chen, K.; Bell, A.T.; Iglesia, E. Kinetics and Mechanism of Oxidative Dehydrogenation of Propane on Vanadium, Molybdenum, and Tungsten Oxides. *J. Phys. Chem. B* **2000**, *104*, 1292–1299. [CrossRef]
102. Argyle, M.D.; Chen, K.; Resini, C.; Krebs, C.; Bell, A.T.; Iglesia, E. Extent of Reduction of Vanadium Oxides during Catalytic Oxidation of Alkanes Measured by In-Situ UV−Visible Spectroscopy. *J. Phys. Chem. B* **2004**, *108*, 2345–2353. [CrossRef]
103. Nguyen, L.; Loridant, S.; Launay, H.; Pigamo, A.; Dubois, J.; Millet, J. Study of New Catalysts Based on Vanadium Oxide Supported on Mesoporous Silica for the Partial Oxidation of Methane to Formaldehyde: Catalytic Properties and Reaction Mechanism. *J. Catal.* **2006**, *237*, 38–48. [CrossRef]
104. Ding, X.L.; Zhao, Y.X.; Wu, X.N.; Wang, Z.C.; Ma, J.B.; He, S.G. Hydrogen-Atom Abstraction from Methane by Stoichiometric Vanadium-Silicon Heteronuclear Oxide Cluster Cations. *Chem.-A Eur. J.* **2010**, *16*, 11463–11470. [CrossRef] [PubMed]
105. Datka, J.; Turek, A.M.; Jehng, J.M.; Wachs, I.E. Acidic Properties of Supported Niobium Oxide Catalysts: An Infrared Spectroscopy Investigation. *J. Catal.* **1992**, *135*, 186–199. [CrossRef]
106. Busca, G.; Ramis, G.; Lorenzelli, V. FT-IR Study of the Surface Properties of Polycrystalline Vanadia. *J. Mol. Catal.* **1989**, *50*, 231–240. [CrossRef]
107. Hu, P.; Lang, W.Z.; Yan, X.; Chen, X.F.; Guo, Y.J. Vanadium-Doped Porous Silica Materials with High Catalytic Activity and Stability for Propane Dehydrogenation Reaction. *Appl. Catal. A Gen.* **2018**, *553*, 65–73. [CrossRef]
108. Xue, X.-L.; Lang, W.-Z.; Yan, X.; Guo, Y.-J. Dispersed Vanadium in Three-Dimensional Dendritic Mesoporous Silica Nanospheres: Active and Stable Catalysts for the Oxidative Dehydrogenation of Propane in the Presence of CO_2. *ACS Appl. Mater. Interfaces* **2017**, *9*, 15408–15423. [CrossRef]
109. Ghampson, I.T.; Lundin, S.-T.B.; Vargheese, V.; Kobayashi, Y.; Huff, G.S.; Schlögl, R.; Trunschke, A.; Oyama, S.T. Methane Selective Oxidation on Metal Oxide Catalysts at Low Temperatures with O_2 Using an NO/NO_2 Oxygen Atom Shuttle. *J. Catal.* **2021**. [CrossRef]
110. Barbero, J.A.; Alvarez, M.C.; Bañares, M.A.; Peña, M.A.; Fierro, J.L.G. Breakthrough in the Direct Conversion of Methane into C1-Oxygenates. *Chem. Commun.* **2002**, *11*, 1184–1185. [CrossRef]
111. Bañares, M.A.; Cardoso, J.H.; Hutchings, G.J.; Bueno, J.M.C.; Fierro, J.L.G. Selective Oxidation of Methane to Methanol and Formaldehyde over V_2O_5/SiO_2 Catalysts. Role of NO in the Gas Phase. *Catal. Lett.* **1998**, *56*, 149–153. [CrossRef]
112. Arena, F.; Giordano, N.; Parmaliana, A. Working Mechanism of Oxide Catalysts in the Partial Oxidation of Methane to Formaldehyde. II. Redox Properties and Reactivity of SiO_2, MoO_3/SiO_2, V_2O_5/SiO_2, TiO_2, and V_2O_5/TiO_2 Systems. *J. Catal.* **1997**, *167*, 66–76. [CrossRef]
113. Wallis, P.; Wohlrab, S.; Kalevaru, V.N.; Frank, M.; Martin, A. Impact of Support Pore Structure and Morphology on Catalyst Performance of VO_x/SBA-15 for Selective Methane Oxidation. *Catal. Today* **2016**, *278*, 120–126. [CrossRef]
114. Du, G.; Yang, Y.; Qiu, W.; Lim, S.; Pfefferle, L.; Haller, G. Statistical Design and Modeling of the Process of Methane Partial Oxidation Using V-MCM-41 Catalysts and the Prediction of the Formaldehyde Production. *Appl. Catal. A Gen.* **2006**, *313*, 1–13. [CrossRef]
115. Dang, T.T.H.; Seeburg, D.; Radnik, J.; Kreyenschulte, C.; Atia, H.; Vu, T.T.H.; Wohlrab, S. Influence of V-Sources on the Catalytic Performance of VMCM-41 in the Selective Oxidation of Methane to Formaldehyde. *Catal. Commun.* **2018**, *103*, 56–59. [CrossRef]
116. Kunkel, B.; Kabelitz, A.; Buzanich, A.G.; Wohlrab, S. Increasing the Efficiency of Optimized V-SBA-15 Catalysts in the Selective Oxidation of Methane to Formaldehyde by Artificial Neural Network Modelling. *Catalysts* **2020**, *10*, 1411. [CrossRef]
117. Zhang, H.; Zhang, J.; Sun, K.; Feng, Z.; Ying, P.; Li, C. Catalytic Performance of the Sb–V Mixed Oxide on Sb–V–O/SiO_2 Catalysts in Methane Selective Oxidation to Formaldehyde. *Catal. Lett.* **2006**, *106*, 89–93. [CrossRef]
118. Battiston, A.A.; Bitter, J.H.; de Groot, F.M.F.; Overweg, A.R.; Stephan, O.; van Bokhoven, J.A.; Kooyman, P.J.; van der Spek, C.; Vankó, G.; Koningsberger, D.C. Evolution of Fe Species during the Synthesis of Over-Exchanged Fe/ZSM-5 Obtained by Chemical Vapor Deposition of $FeCl_3$. *J. Catal.* **2003**, *213*, 251–271. [CrossRef]
119. Marturano, P.; Drozdová, L.; Kogelbauer, A.; Prins, R. Fe/ZSM-5 Prepared by Sublimation of $FeCl_3$: The Structure of the Fe Species as Determined by IR, ^{27}Al MAS NMR, and EXAFS Spectroscopy. *J. Catal.* **2000**, *192*, 236–247. [CrossRef]
120. Kobayashi, T.; Guilhaume, N.; Miki, J.; Kitamura, N.; Haruta, M. Oxidation of Methane to Formaldehyde over Fe/SiO_2 and Sn-W Mixed Oxides. *Catal. Today* **1996**, *32*, 171–175. [CrossRef]

121. Zhang, Q.; Yang, W.; Wang, X.; Wang, Y.; Shishido, T.; Takehira, K. Coordination Structures of Vanadium and Iron in MCM-41 and the Catalytic Properties in Partial Oxidation of Methane. *Microporous Mesoporous Mater.* **2005**, *77*, 223–234. [CrossRef]
122. Ertl, G.; Knözinger, H.; Weitkamp, J. *Handbook of Heterogeneous Catalysis*; Wiley-VCH Verlag GmbH: Hoboken, NJ, USA, 2008; Volumes 1–5, ISBN 9783527619474.
123. He, J.; Li, Y.; An, D.; Zhang, Q.; Wang, Y. Selective Oxidation of Methane to Formaldehyde by Oxygen over Silica-Supported Iron Catalysts. *J. Nat. Gas Chem.* **2009**, *18*, 288–294. [CrossRef]
124. McCormick, R.L.; Alptekin, G.O.; Williamson, D.L.; Ohno, T.R. Methane Partial Oxidation by Silica-supported Iron Phosphate Catalysts. Influence of Iron Phosphate Content on Selectivity and Catalyst Structure. *Top. Catal.* **2000**, *10*, 115–122. [CrossRef]
125. Alptekin, G.O.; Herring, A.M.; Williamson, D.L.; Ohno, T.R.; McCormick, R.L. Methane Partial Oxidation by Unsupported and Silica Supported Iron Phosphate Catalysts. *J. Catal.* **1999**, *181*, 104–112. [CrossRef]
126. Cortés Ortiz, W.G.; Delgado, D.; Guerrero Fajardo, C.A.; Agouram, S.; Sanchís, R.; Solsona, B.; López Nieto, J.M. Partial Oxidation of Methane and Methanol on FeO_x-, MoO_x- and $FeMoO_x$-SiO_2 Catalysts Prepared by Sol-Gel Method: A Comparative Study. *Mol. Catal.* **2020**, *491*, 110982. [CrossRef]
127. Kanai, S.; Nagahara, I.; Kita, Y.; Kamata, K.; Hara, M. A Bifunctional Cerium Phosphate Catalyst for Chemoselective Acetalization. *Chem. Sci.* **2017**, *8*, 3146–3153. [CrossRef] [PubMed]
128. Sato, A.; Ogo, S.; Kamata, K.; Takeno, Y.; Yabe, T.; Yamamoto, T.; Matsumura, S.; Hara, M.; Sekine, Y. Ambient-Temperature Oxidative Coupling of Methane in an Electric Field by a Cerium Phosphate Nanorod Catalyst. *Chem. Commun.* **2019**, *55*, 4019–4022. [CrossRef] [PubMed]
129. Krisnandi, Y.K.; Nurani, D.A.; Alfian, D.V.; Sofyani, U.; Faisal, M.; Saragi, I.R.; Pamungkas, A.Z.; Pratama, A.P. The New Challenge of Partial Oxidation of Methane over Fe_2O_3/NaY and Fe_3O_4/NaY Heterogeneous Catalysts. *Heliyon* **2021**, *7*, e08305. [CrossRef]
130. Gomonaj, V.; Toulhoat, H. Selective Oxidation of Methane to Formaldehyde Catalyzed by Phosphates: Kinetic Description by Bond Strengths and Specific Total Acidities. *ACS Catal.* **2018**, *8*, 8263–8272. [CrossRef]
131. Dasireddy, V.D.B.C.; Hanzel, D.; Bharuth-Ram, K.; Likozar, B. The Effect of Oxidant Species on Direct, Non-Syngas Conversion of Methane to Methanol over an $FePO_4$ Catalyst Material. *RSC Adv.* **2019**, *9*, 30989–31003. [CrossRef]
132. Paunović, V.; Zichittella, G.; Moser, M.; Amrute, A.P.; Pérez-Ramírez, J. Catalyst Design for Natural-Gas Upgrading through Oxybromination Chemistry. *Nat. Chem.* **2016**, *8*, 803–809. [CrossRef]
133. Zichittella, G.; Paunović, V.; Amrute, A.P.; Pérez-Ramírez, J. Catalytic Oxychlorination versus Oxybromination for Methane Functionalization. *ACS Catal.* **2017**, *7*, 1805–1817. [CrossRef]
134. Bozbag, S.E.; Alayon, E.M.C.; Pecháček, J.; Nachtegaal, M.; Ranocchiari, M.; van Bokhoven, J.A. Methane to Methanol over Copper Mordenite: Yield Improvement through Multiple Cycles and Different Synthesis Techniques. *Catal. Sci. Technol.* **2016**, *6*, 5011–5022. [CrossRef]
135. Le, H.v.; Parishan, S.; Sagaltchik, A.; Göbel, C.; Schlesiger, C.; Malzer, W.; Trunschke, A.; Schomäcker, R.; Thomas, A. Solid-State Ion-Exchanged Cu/Mordenite Catalysts for the Direct Conversion of Methane to Methanol. *ACS Catal.* **2017**, *7*, 1403–1412. [CrossRef]
136. Ipek, B.; Wulfers, M.J.; Kim, H.; Göltl, F.; Hermans, I.; Smith, J.P.; Booksh, K.S.; Brown, C.M.; Lobo, R.F. Formation of $[Cu_2O_2]^{2+}$ and $[Cu_2O]^{2+}$ toward C–H Bond Activation in Cu-SSZ-13 and Cu-SSZ-39. *ACS Catal.* **2017**, *7*, 4291–4303. [CrossRef]
137. Wulfers, M.J.; Teketel, S.; Ipek, B.; Lobo, R.F. Conversion of Methane to Methanol on Copper-Containing Small-Pore Zeolites and Zeotypes. *Chem. Commun.* **2015**, *51*, 4447–4450. [CrossRef] [PubMed]
138. Beznis, N.v.; Weckhuysen, B.M.; Bitter, J.H. Cu-ZSM-5 Zeolites for the Formation of Methanol from Methane and Oxygen: Probing the Active Sites and Spectator Species. *Catal. Lett.* **2010**, *138*, 14–22. [CrossRef]
139. An, D.; Zhang, Q.; Wang, Y. Copper Grafted on SBA-15 as Efficient Catalyst for the Selective Oxidation of Methane by Oxygen. *Catal. Today* **2010**, *157*, 143–148. [CrossRef]
140. Kim, D.S.; Ostromecki, M.; Wachs, I.E.; Kohler, S.D.; Ekerdt, J.G. Preparation and Characterization of WO_3/SiO_2 Catalysts. *Catal. Lett.* **1995**, *33*, 209–215. [CrossRef]
141. Kohler, S.D.; Ekerdt, J.G.; Kim, D.S.; Wachs, I.E. Relationship between Structure and Point of Zero Surface Charge for Molybdenum and Tungsten Oxides Supported on Alumina. *Catal. Lett.* **1992**, *16*, 231–239. [CrossRef]
142. De Lucas, A.; Valverde, J.L.; Cañizares, P.; Rodriguez, L. Partial Oxidation of Methane to Formaldehyde over W/SiO_2 Catalysts. *Appl. Catal. A Gen.* **1999**, *184*, 143–152. [CrossRef]
143. Krisnandi, Y.K.; Putra, B.A.P.; Bahtiar, M.; Zahara; Abdullah, I.; Howe, R.F. Partial Oxidation of Methane to Methanol over Heterogeneous Catalyst Co/ZSM-5. *Procedia Chem.* **2015**, *14*, 508–515. [CrossRef]
144. Beznis, N.v.; van Laak, A.N.C.; Weckhuysen, B.M.; Bitter, J.H. Oxidation of Methane to Methanol and Formaldehyde over Co–ZSM-5 Molecular Sieves: Tuning the Reactivity and Selectivity by Alkaline and Acid Treatments of the Zeolite ZSM-5 Agglomerates. *Microporous Mesoporous Mater.* **2011**, *138*, 176–183. [CrossRef]
145. Shi, L.; Wang, Y.; Yan, B.; Song, W.; Shao, D.; Lu, A.H. Progress in Selective Oxidative Dehydrogenation of Light Alkanes to Olefins Promoted by Boron Nitride Catalysts. *Chem. Commun.* **2018**, *54*, 10936–10946. [CrossRef] [PubMed]
146. Venegas, J.M.; McDermott, W.P.; Hermans, I. Serendipity in Catalysis Research: Boron-Based Materials for Alkane Oxidative Dehydrogenation. *Acc. Chem. Res.* **2018**, *51*, 2556–2564. [CrossRef]
147. Atroshchenko, V.I.; Shchedrinskaya, Z.M.; Gavrya, N.A. Catalysts for the Oxidation of Natural Gas to Formaldehyde and Methanol. *Zhurnal Prikl. Khimii* **1965**, *38*, 643–649.

148. Dowden, D.A.; Walker, G.T. Oxygenated Hydrocarbons Production. British Patent 1,244,001, 25 August 1971. Available online: https://patents.google.com/patent/GB1244001A/en (accessed on 14 February 2022).
149. Zhang, X.; He, D.; Zhang, Q.; Xu, B.; Zhu, Q. Comparative Studies on Direct Conversion of Methane to Methanol/Formaldehyde over La-Co-O and ZrO_2 Supported Molybdenum Oxide Catalysts. *Top. Catal.* **2005**, *32*, 215–223. [CrossRef]
150. Sugino, T.; Kido, A.; Azuma, N.; Ueno, A.; Udagawa, Y. Partial Oxidation of Methane on Silica-Supported Silicomolybdic Acid Catalysts in an Excess Amount of Water Vapor. *J. Catal.* **2000**, *190*, 118–127. [CrossRef]
151. Liu, R.-S.; Iwamoto, M.; Lunsford, J.H. Partial Oxidation of Methane by Nitrous Oxide over Molybdenum Oxide Supported on Silica. *J. Chem. Soc. Chem. Commun.* **1982**, *78*. [CrossRef]
152. Chen, S.Y.; Willcox, D. Effect of Vanadium Oxide Loading on the Selective Oxidation of Methane over Vanadium Oxide (V_2O_5)/Silica. *Ind. Eng. Chem. Res.* **1993**, *32*, 584–587. [CrossRef]
153. Sun, L.; Wang, Y.; Wang, C.; Xie, Z.; Guan, N.; Li, L. Water-Involved Methane-Selective Catalytic Oxidation by Dioxygen over Copper Zeolites. *Chem* **2021**, *7*, 1557–1568. [CrossRef]
154. Dinh, K.T.; Sullivan, M.M.; Narsimhan, K.; Serna, P.; Meyer, R.J.; Dincă, M.; Román-Leshkov, Y. Continuous Partial Oxidation of Methane to Methanol Catalyzed by Diffusion-Paired Copper Dimers in Copper-Exchanged Zeolites. *J. Am. Chem. Soc.* **2019**, *141*, 11641–11650. [CrossRef] [PubMed]
155. Jeong, Y.R.; Jung, H.; Kang, J.; Han, J.W.; Park, E.D. Continuous Synthesis of Methanol from Methane and Steam over Copper-Mordenite. *ACS Catal.* **2021**, *11*, 1065–1070. [CrossRef]
156. Dasireddy, V.D.B.C.; Likozar, B. Direct Methanol Production from Mixed Methane/H_2O/N_2O Feedstocks over Cu–Fe/Al_2O_3 Catalysts. *Fuel* **2021**, *301*, 121084. [CrossRef]
157. Li, Y.; Liu, N.; Dai, C.; Xu, R.; Yu, G.; Wang, N.; Zhang, J.; Chen, B. Synergistic Effect of Neighboring Fe and Cu Cation Sites Boosts FenCum-BEA Activity for the Continuous Direct Oxidation of Methane to Methanol. *Catalysts* **2021**, *11*, 1444. [CrossRef]
158. Wang, H.; Xin, W.; Wang, Q.; Zheng, X.; Lu, Z.; Pei, R.; He, P.; Dong, X. Direct Methane Conversion with Oxygen and CO over Hydrophobic DB-ZSM-5 Supported Rh Single-Atom Catalyst. *Catal. Commun.* **2022**, *162*, 106374. [CrossRef]
159. Lyu, Y.; Jocz, J.N.; Xu, R.; Williams, O.C.; Sievers, C. Selective Oxidation of Methane to Methanol over Ceria-Zirconia Supported Mono and Bimetallic Transition Metal Oxide Catalysts. *ChemCatChem* **2021**, *13*, 2832–2842. [CrossRef]
160. Memioglu, O.; Ipek, B. A Potential Catalyst for Continuous Methane Partial Oxidation to Methanol Using N_2O: Cu-SSZ-39. *Chem. Commun.* **2021**, *57*, 1364–1367. [CrossRef]
161. Lee, S.H.; Kang, J.K.; Park, E.D. Continuous Methanol Synthesis Directly from Methane and Steam over Cu(II)-Exchanged Mordenite. *Korean J. Chem. Eng.* **2018**, *35*, 2145–2149. [CrossRef]
162. Huang, E.; Orozco, I.; Ramírez, P.J.; Liu, Z.; Zhang, F.; Mahapatra, M.; Nemšák, S.; Senanayake, S.D.; Rodriguez, J.A.; Liu, P. Selective Methane Oxidation to Methanol on ZnO/Cu_2O/Cu(111) Catalysts: Multiple Site-Dependent Behaviors. *J. Am. Chem. Soc.* **2021**, *143*, 19018–19032. [CrossRef]
163. Hirayama, A.; Tsuchimura, Y.; Yoshida, H.; Machida, M.; Nishimura, S.; Kato, K.; Takahashi, K.; Ohyama, J. Catalytic Oxidation of Methane to Methanol over Cu-CHA with Molecular Oxygen. *Catal. Sci. Technol.* **2021**, *11*, 6217–6224. [CrossRef]
164. Arutyunov, V.S.; Basevich, V.Y.; Vedeneev, V.I. Direct High-Pressure Gas-Phase Oxidation of Natural Gas to Methanol and Other Oxygenates. *Russ. Chem. Rev.* **1996**, *65*, 197–224. [CrossRef]
165. Panov, G.I.; Sobolev, V.I.; Dubkov, K.A.; Parmon, V.N.; Ovanesyan, N.S.; Shilov, A.E.; Shteinman, A.A. Iron Complexes in Zeolites as a New Model of Methane Monooxygenase. *React. Kinet. Catal. Lett.* **1997**, *61*, 251–258. [CrossRef]
166. Sushkevich, V.L.; van Bokhoven, J.A. Methane-to-Methanol: Activity Descriptors in Copper-Exchanged Zeolites for the Rational Design of Materials. *ACS Catal.* **2019**, *9*, 6293–6304. [CrossRef]
167. Sobolev, V.I.; Dubkov, K.A.; Panna, O.v.; Panov, G.I. Selective Oxidation of Methane to Methanol on a FeZSM-5 Surface. *Catal. Today* **1995**, *24*, 251–252. [CrossRef]
168. Zhu, J.; Liang, W.; Erik, Z.; Kartick, M.; Zhang, M.; Zhang, J.; Wang, C.; Meng, X.; Yang, H.; Carl, M.; et al. Hydrophobic Zeolite Modification for in Situ Peroxide Formation in Methane Oxidation to Methanol. *Science* **2020**, *367*, 193–197. [CrossRef]
169. Narsimhan, K.; Iyoki, K.; Dinh, K.; Román-Leshkov, Y. Catalytic Oxidation of Methane into Methanol over Copper-Exchanged Zeolites with Oxygen at Low Temperature. *ACS Cent. Sci.* **2016**, *2*, 424–429. [CrossRef]
170. Mahyuddin, M.H.; Tanaka, T.; Shiota, Y.; Staykov, A.; Yoshizawa, K. Methane Partial Oxidation over $[Cu_2(\mu\text{-}O)]^{2+}$ and $[Cu_3(\mu\text{-}O)_3]^{2+}$ Active Species in Large-Pore Zeolites. *ACS Catal.* **2018**, *8*, 1500–1509. [CrossRef]
171. Dyballa, M.; Pappas, D.K.; Kvande, K.; Borfecchia, E.; Arstad, B.; Beato, P.; Olsbye, U.; Svelle, S. On How Copper Mordenite Properties Govern the Framework Stability and Activity in the Methane-to-Methanol Conversion. *ACS Catal.* **2019**, *9*, 365–375. [CrossRef]
172. Xie, J.; Jin, R.; Li, A.; Bi, Y.; Ruan, Q.; Deng, Y.; Zhang, Y.; Yao, S.; Sankar, G.; Ma, D.; et al. Highly Selective Oxidation of Methane to Methanol at Ambient Conditions by Titanium Dioxide-Supported Iron Species. *Nat. Catal.* **2018**, *1*, 889–896. [CrossRef]
173. Cui, X.; Li, H.; Wang, Y.; Hu, Y.; Hua, L.; Li, H.; Han, X.; Liu, Q.; Yang, F.; He, L.; et al. Room-Temperature Methane Conversion by Graphene-Confined Single Iron Atoms. *Chem* **2018**, *4*, 1902–1910. [CrossRef]
174. Wood, B.R.; Reimer, J.A.; Bell, A.T.; Janicke, M.T.; Ott, K.C. Methanol Formation on Fe/Al-MFI via the Oxidation of Methane by Nitrous Oxide. *J. Catal.* **2004**, *225*, 300–306. [CrossRef]
175. Pannov, G.I.; Sobolev, V.I.; Kharitonov, A.S. The Role of Iron in N_2O Decomposition on ZSM-5 Zeolite and Reactivity of the Surface Oxygen Formed. *J. Mol. Catal.* **1990**, *61*, 85–97. [CrossRef]

176. Starokon, E.v.; Parfenov, M.v.; Arzumanov, S.S.; Pirutko, L.v.; Stepanov, A.G.; Panov, G.I. Oxidation of Methane to Methanol on the Surface of FeZSM-5 Zeolite. *J. Catal.* **2013**, *300*, 47–54. [CrossRef]
177. Starokon, E.v.; Parfenov, M.v.; Pirutko, L.v.; Abornev, S.I.; Panov, G.I. Room-Temperature Oxidation of Methane by α-Oxygen and Extraction of Products from the FeZSM-5 Surface. *J. Phys. Chem. C* **2011**, *115*, 2155–2161. [CrossRef]
178. Snyder, B.E.R.; Vanelderen, P.; Bols, M.L.; Hallaert, S.D.; Böttger, L.H.; Ungur, L.; Pierloot, K.; Schoonheydt, R.A.; Sels, B.F.; Solomon, E.I. The Active Site of Low-Temperature Methane Hydroxylation in Iron-Containing Zeolites. *Nature* **2016**, *536*, 317–321. [CrossRef] [PubMed]
179. Bols, M.L.; Devos, J.; Rhoda, H.M.; Plessers, D.; Solomon, E.I.; Schoonheydt, R.A.; Sels, B.F.; Dusselier, M. Selective Formation of α-Fe(II) Sites on Fe-Zeolites through One-Pot Synthesis. *J. Am. Chem. Soc.* **2021**, *143*, 16243–16255. [CrossRef] [PubMed]
180. Bols, M.L.; Snyder, B.E.R.; Rhoda, H.M.; Cnudde, P.; Fayad, G.; Schoonheydt, R.A.; van Speybroeck, V.; Solomon, E.I.; Sels, B.F. Coordination and Activation of Nitrous Oxide by Iron Zeolites. *Nat. Catal.* **2021**, *4*, 332–340. [CrossRef]
181. Snyder, B.E.R.; Bol, M.L.; Rhoda, H.M.; Plessers, D.; Schoonheydt, R.A.; Sels, B.F.; Solomon, E.I. Cage Effects Control the Mechanism of Methane Hydroxylation in Zeolites. *Science* **2021**, *373*, 327–331. [CrossRef]
182. Zhao, G.; Benhelal, E.; Adesina, A.; Kennedy, E.; Stockenhuber, M. Comparison of Direct, Selective Oxidation of Methane by N_2O over Fe-ZSM-5, Fe-Beta, and Fe-FER Catalysts. *J. Phys. Chem. C* **2019**, *123*, 27436–27447. [CrossRef]
183. Parfenov, M.v.; Starokon, E.v.; Pirutko, L.v.; Panov, G.I. Quasicatalytic and Catalytic Oxidation of Methane to Methanol by Nitrous Oxide over FeZSM-5 Zeolite. *J. Catal.* **2014**, *318*, 14–21. [CrossRef]
184. Li, S.; Fan, L.; Song, L.; Cheng, D.; Chen, F. Influence of Extra-Framework Al in Fe-MOR Catalysts for the Direct Conversion of Methane to Oxygenates by Nitrous Oxide. *Chin. J. Chem. Eng.* **2021**, *33*, 132–138. [CrossRef]
185. Zhao, G.; Adesina, A.; Kennedy, E.; Stockenhuber, M. Formation of Surface Oxygen Species and the Conversion of Methane to Value-Added Products with N_2O as Oxidant over Fe-Ferrierite Catalysts. *ACS Catal.* **2020**, *10*, 1406–1416. [CrossRef]
186. Simons, M.C.; Prinslow, S.D.; Babucci, M.; Hoffman, A.S.; Hong, J.; Vitillo, J.G.; Bare, S.R.; Gates, B.C.; Lu, C.C.; Gagliardi, L.; et al. Beyond Radical Rebound: Methane Oxidation to Methanol Catalyzed by Iron Species in Metal–Organic Framework Nodes. *J. Am. Chem. Soc.* **2021**, *143*, 12165–12174. [CrossRef] [PubMed]
187. Park, M.B.; Park, E.D.; Ahn, W.-S. Recent Progress in Direct Conversion of Methane to Methanol Over Copper-Exchanged Zeolites. *Front. Chem.* **2019**, *7*, 514. [CrossRef]
188. Mahyuddin, M.H.; Shiota, Y.; Staykov, A.; Yoshizawa, K. Theoretical Overview of Methane Hydroxylation by Copper–Oxygen Species in Enzymatic and Zeolitic Catalysts. *Acc. Chem. Res.* **2018**, *51*, 2382–2390. [CrossRef] [PubMed]
189. Sushkevich, V.L.; Artsiusheuski, M.; Klose, D.; Jeschke, G.; van Bokhoven, J.A. Identification of Kinetic and Spectroscopic Signatures of Copper Sites for Direct Oxidation of Methane to Methanol. *Angew. Chem. Int. Ed.* **2021**, *60*, 15944–15953. [CrossRef] [PubMed]
190. Tomkins, P.; Ranocchiari, M.; van Bokhoven, J.A. Direct Conversion of Methane to Methanol under Mild Conditions over Cu-Zeolites and Beyond. *Acc. Chem. Res.* **2017**, *50*, 418–425. [CrossRef] [PubMed]
191. Snyder, B.E.R.; Bols, M.L.; Schoonheydt, R.A.; Sels, B.F.; Solomon, E.I. Iron and Copper Active Sites in Zeolites and Their Correlation to Metalloenzymes. *Chem. Rev.* **2018**, *118*, 2718–2768. [CrossRef] [PubMed]
192. Groothaert, M.H.; Smeets, P.J.; Sels, B.F.; Jacobs, P.A.; Schoonheydt, R.A. Selective Oxidation of Methane by the Bis(μ-Oxo)Dicopper Core Stabilized on ZSM-5 and Mordenite Zeolites. *J. Am. Chem. Soc.* **2005**, *127*, 1394–1395. [CrossRef] [PubMed]
193. Woertink, J.S.; Smeets, P.J.; Groothaert, M.H.; Vance, M.A.; Sels, B.F.; Schoonheydt, R.A.; Solomon, E.I. A $[Cu_2\ O]^{2+}$ Core in Cu-ZSM-5, the Active Site in the Oxidation of Methane to Methanol. *Proc. Natl. Acad. Sci. USA* **2009**, *106*, 18908–18913. [CrossRef]
194. Li, G.; Vassilev, P.; Sanchez-Sanchez, M.; Lercher, J.A.; Hensen, E.J.M.; Pidko, E.A. Stability and Reactivity of Copper Oxo-Clusters in ZSM-5 Zeolite for Selective Methane Oxidation to Methanol. *J. Catal.* **2016**, *338*, 305–312. [CrossRef]
195. Grundner, S.; Markovits, M.A.C.; Li, G.; Tromp, M.; Pidko, E.A.; Hensen, E.J.M.; Jentys, A.; Sanchez-Sanchez, M.; Lercher, J.A. Single-Site Trinuclear Copper Oxygen Clusters in Mordenite for Selective Conversion of Methane to Methanol. *Nat. Commun.* **2015**, *6*, 7546. [CrossRef]
196. Vanelderen, P.; Snyder, B.E.R.; Tsai, M.L.; Hadt, R.G.; Vancauwenbergh, J.; Coussens, O.; Schoonheydt, R.A.; Sels, B.F.; Solomon, E.I. Spectroscopic Definition of the Copper Active Sites in Mordenite: Selective Methane Oxidation. *J. Am. Chem. Soc.* **2015**, *137*, 6383–6392. [CrossRef] [PubMed]
197. Kim, Y.; Kim, T.Y.; Lee, H.; Yi, J. Distinct Activation of Cu-MOR for Direct Oxidation of Methane to Methanol. *Chem. Commun.* **2017**, *53*, 4116–4119. [CrossRef] [PubMed]
198. Ipek, B.; Lobo, R.F. Catalytic Conversion of Methane to Methanol on Cu-SSZ-13 Using N_2O as Oxidant. *Chem. Commun.* **2016**, *52*, 13401–13404. [CrossRef] [PubMed]
199. Tomkins, P.; Mansouri, A.; Sushkevich, V.L.; van der Wal, L.I.; Bozbag, S.E.; Krumeich, F.; Ranocchiari, M.; van Bokhoven, J.A. Increasing the Activity of Copper Exchanged Mordenite in the Direct Isothermal Conversion of Methane to Methanol by Pt and Pd Doping. *Chem. Sci.* **2019**, *10*, 167–171. [CrossRef] [PubMed]
200. Bozbag, S.E.; Sot, P.; Nachtegaal, M.; Ranocchiari, M.; van Bokhoven, J.A.; Mesters, C. Direct Stepwise Oxidation of Methane to Methanol over Cu–SiO_2. *ACS Catal.* **2018**, *8*, 5721–5731. [CrossRef]
201. Elwell, C.E.; Gagnon, N.L.; Neisen, B.D.; Dhar, D.; Spaeth, A.D.; Yee, G.M.; Tolman, W.B. Copper–Oxygen Complexes Revisited: Structures, Spectroscopy, and Reactivity. *Chem. Rev.* **2017**, *117*, 2059–2107. [CrossRef]

202. Kulkarni, A.R.; Zhao, Z.-J.; Siahrostami, S.; Nørskov, J.K.; Studt, F. Cation-Exchanged Zeolites for the Selective Oxidation of Methane to Methanol. *Catal. Sci. Technol.* **2018**, *8*, 114–123. [CrossRef]
203. Lange, J.-P.; Sushkevich, V.L.; Knorpp, A.J.; van Bokhoven, J.A. Methane-to-Methanol via Chemical Looping: Economic Potential and Guidance for Future Research. *Ind. Eng. Chem. Res.* **2019**, *58*, 8674–8680. [CrossRef]
204. Alayon, E.M.; Nachtegaal, M.; Ranocchiari, M.; van Bokhoven, J.A. Catalytic Conversion of Methane to Methanol over Cu–Mordenite. *Chem. Commun.* **2012**, *48*, 404–406. [CrossRef]
205. Sushkevich, V.L.; Palagin, D.; Ranocchiari, M.; van Bokhoven, J.A. Selective Anaerobic Oxidation of Methane Enables Direct Synthesis of Methanol. *Science* **2017**, *356*, 523–527. [CrossRef]
206. Sushkevich, V.L.; Palagin, D.; van Bokhoven, J.A. The Effect of the Active-Site Structure on the Activity of Copper Mordenite in the Aerobic and Anaerobic Conversion of Methane into Methanol. *Angew. Chem.* **2018**, *130*, 9044–9048. [CrossRef]
207. Pappas, D.K.; Martini, A.; Dyballa, M.; Kvande, K.; Teketel, S.; Lomachenko, K.A.; Baran, R.; Glatzel, P.; Arstad, B.; Berlier, G.; et al. The Nuclearity of the Active Site for Methane to Methanol Conversion in Cu-Mordenite: A Quantitative Assessment. *J. Am. Chem. Soc.* **2018**, *140*, 15270–15278. [CrossRef] [PubMed]
208. Pappas, D.K.; Borfecchia, E.; Dyballa, M.; Pankin, I.A.; Lomachenko, K.A.; Martini, A.; Signorile, M.; Teketel, S.; Arstad, B.; Berlier, G.; et al. Methane to Methanol: Structure–Activity Relationships for Cu-CHA. *J. Am. Chem. Soc.* **2017**, *139*, 14961–14975. [CrossRef] [PubMed]
209. Markovits, M.A.C.; Jentys, A.; Tromp, M.; Sanchez-Sanchez, M.; Lercher, J.A. Effect of Location and Distribution of Al Sites in ZSM-5 on the Formation of Cu-Oxo Clusters Active for Direct Conversion of Methane to Methanol. *Top. Catal.* **2016**, *59*, 1554–1563. [CrossRef]
210. Brezicki, G.; Zheng, J.; Paolucci, C.; Schlögl, R.; Davis, R.J. Effect of the Co-Cation on Cu Speciation in Cu-Exchanged Mordenite and ZSM-5 Catalysts for the Oxidation of Methane to Methanol. *ACS Catal.* **2021**, *11*, 4973–4987. [CrossRef]
211. Zhou, C.; Zhang, H.; Yang, L.; Wu, D.; He, S.; Yang, H.; Xiong, H. Methane-Selective Oxidation to Methanol and Ammonia Selective Catalytic Reduction of NO_x over Monolithic Cu/SSZ-13 Catalysts: Are Hydrothermal Stability and Active Sites Same? *Fuel* **2022**, *309*, 122178. [CrossRef]
212. Xiong, H.; Zhang, H.; Lv, J.; Zhang, Z.; Du, C.; Wang, S.; Lin, J.; Wan, S.; Wang, Y. Oxidation of Methane to Methanol by Water over Cu/SSZ-13: Impact of Cu Loading and Formation of Active Sites. *ChemCatChem* **2022**, *14*, e202101609. [CrossRef]
213. Park, M.B.; Ahn, S.H.; Mansouri, A.; Ranocchiari, M.; van Bokhoven, J.A. Comparative Study of Diverse Copper Zeolites for the Conversion of Methane into Methanol. *ChemCatChem* **2017**, *9*, 3705–3713. [CrossRef]
214. Knorpp, A.J.; Newton, M.A.; Sushkevich, V.L.; Zimmermann, P.P.; Pinar, A.B.; van Bokhoven, J.A. The Influence of Zeolite Morphology on the Conversion of Methane to Methanol on Copper-Exchanged Omega Zeolite (MAZ). *Catal. Sci. Technol.* **2019**, *9*, 2806–2811. [CrossRef]
215. Lee, I.; Lee, M.-S.; Tao, L.; Ikuno, T.; Khare, R.; Jentys, A.; Huthwelker, T.; Borca, C.N.; Kalinko, A.; Gutiérrez, O.Y.; et al. Activity of Cu–Al–Oxo Extra-Framework Clusters for Selective Methane Oxidation on Cu-Exchanged Zeolites. *JACS Au* **2021**, *1*, 1412–1421. [CrossRef]
216. Shan, J.; Huang, W.; Nguyen, L.; Yu, Y.; Zhang, S.; Li, Y.; Frenkel, A.I.; Tao, F. Conversion of Methane to Methanol with a Bent Mono(μ-Oxo)Dinickel Anchored on the Internal Surfaces of Micropores. *Langmuir* **2014**, *30*, 8558–8569. [CrossRef] [PubMed]
217. Mlekodaj, K.; Lemishka, M.; Sklenak, S.; Dedecek, J.; Tabor, E. Dioxygen Splitting at Room Temperature over Distant Binuclear Transition Metal Centers in Zeolites for Direct *Oxid.* of Methane to Methanol. *Chem. Commun.* **2021**, *57*, 3472–3475. [CrossRef] [PubMed]
218. Fu, L.; Yuan, M.; Li, X.; Bian, S.; Mi, L.; Gao, Z.; Shi, Q.; Huang, W.; Zuo, Z. The Influence of UiO-bpy Skeleton for the Direct Methane-to-Methanol Conversion on Cu@UiO-bpy: Importance of the Encapsulation Effect. *ChemCatChem* **2021**, *13*, 4897–4902. [CrossRef]
219. Jovanovic, Z.R.; Lange, J.-P.; Ravi, M.; Knorpp, A.J.; Sushkevich, V.L.; Newton, M.A.; Palagin, D.; van Bokhoven, J.A. Oxidation of Methane to Methanol over Cu-Exchanged Zeolites: Scientia Gratia Scientiae or Paradigm Shift in Natural Gas Valorization? *J. Catal.* **2020**, *385*, 238–245. [CrossRef]